INVESTIGATION OF BOUNDARIES FOR TRANSITIONS FROM AXIAL TO TWO-DIMENSIONAL FLOW BY ELECTRICAL ANALOGY

Thesis by

Marc Kampé de Fériet

In Partial Fulfillment of the Requirements

for the Degree of

Mechanical Engineer

California Institute of Technology

Pasadena, California

1953

ACKNOWLEDGEMENTS

The writer wishes to thank Professor M. S. Plesset for suggesting this investigation and Profs. A. Hollander, C. Wilts and Dr. A. Acosta for their help during the progress of the work.

ABSTRACT

A study on a series of axially symmetric potential flows in radial-flow impeller channels has been made with the aid of an electrical analogy. An electrolytic tank was built and tested with flows for which the mathematical solution was known. The experimental determination of velocity along the boundaries was within one percent of the exact value.

Velocity distributions on families of impeller channels with ellipsoidal boundaries were then obtained. The parameters varied were inlet to outlet area ratio and eccentricity of the bounding ellipses. These results are presented as graphs and in addition the maximum velocity along the front shroud is given as a function of the various parameters.

This analogy was also applied to a well designed commercial impeller channel and the results compared to the preceding study.

TABLE OF CONTENTS

NOTATIONS

a_1, a_2	semi-axes of the front shroud ellipse
a_1', a_2'	semi-axes of the back shroud ellipse
A_1	inlet section area
A_2	outlet area at radius
C	concentration of the electrolyte
d	spacing of two probes
$\bar{E}$	electric field vector
$\bar{j}$	electric current vector
$i = \sqrt{-1}$	
$\bar{\iota}_1, \bar{\iota}_2, \bar{\iota}_3$	unit vectors of the x, y, z axes
r_1, r_2	inside and outside diameters of the impeller
R	resistance
s	linear distance along the boundary
V	electric potential
v_r, v_z	radial and axial velocities
$\bar{v}$	velocity vector
X_i	reactance
Z	impedance
φ	velocity potential
Ψ	stream function
σ	conductivity of the electrolyte
Λ	molal conductance of the electrolyte
$\bar{\Omega}$	vortex vector

I. GENERAL CONSIDERATIONS

In radial flow turbomachinery, the impeller flow channel changes gradually from an axial to a radial direction. The boundaries are surfaces of revolution so that the axial end is a cylinder and the radial end substantially consists of two parallel planes a short distance apart. This transition from the axial to radial direction is rather sudden and it is important to avoid high local velocities and corresponding low pressures where there might be a danger of cavitation or flow separation. In any event the meridional velocity distribution must be known in order to design properly the inlet angles of the impeller blades.

To actually design or investigate such transitions using the hydrodynamics of viscous fluids is very difficult; therefore this study has been restricted to frictionless flows which will give a good picture of the velocity distribution in the actual real fluid case providing the flow does not separate and the boundary layer is thin. This restriction made it also possible to investigate separately the meridional and rotational components of the flow. Consequently the present study has been restricted to the investigation of the meridional flow in the space of revolution defined by the transition boundary.

Since it is possible, to some extent, to find the influence of the impeller vanes on the meridional flow (Ref. 1), the results obtained here can be applied to the frictionless flow in pumps or turbines.

Even with the simplifications introduced, it is difficult to find the potential function analytically (that is, to solve Laplace's equation with given boundary conditions). It was therefore decided to investigate

experimentally the influence of the transition curve on the velocity distribution in the flow.

This study might have been carried out by at least three different methods; namely,

1. Relaxation method (that is, numerical analysis)
2. Equivalent network analogy
3. Electrical analog

Of these three methods, the third is the simplest and the most suitable for a systematic study. The three-dimensional electrical analog method has been used quite successfully at the Iowa Institute for Hydraulic Research for systematic studies of conduit contractions (Ref. 2).

It was therefore decided to investigate this potential problem by electrical analog.

II. THEORY OF THE ELECTRICAL ANALOG TANK

The fact that an electrolytic tank can be used to solve potential problems is well known. The elements of this analog will be briefly reviewed here.

1. The electric potential V satisfies Laplace's equation in an isotropic conducting medium under steady conditions.

This can be shown easily, for if σ is the conductivity of the conductor, and $\bar{J}$ and $\bar{E}$ are the electric current and field vectors respectively, then Ohm's Law may be stated in vector notations as

$$\bar{J} = \sigma \bar{E} \quad .$$

Since $\bar{E} = -\nabla V$, where ∇ is the operator $\bar{i}_1 \frac{\partial}{\partial x} + \bar{i}_2 \frac{\partial}{\partial y} + \bar{i}_3 \frac{\partial}{\partial z}$, then $\bar{J} = -\sigma \nabla V$; and by the use of the continuity equation $\nabla \cdot \bar{J} = 0$, we get

$$\nabla^2 V = 0$$

where ∇^2 is the Laplacian operator.

2. The velocity potential φ satisfies Laplace's equation for a steady, irrotational flow of a perfect fluid.

The irrotationality condition $\bar{\Omega} = \nabla \times \bar{v} = 0$ implies $\bar{v} = \nabla \varphi$, and by the use of the continuity relation $\nabla \cdot \bar{v} = 0$, we get

$$\nabla^2 \varphi = 0 \quad .$$

We see that both the velocity potential φ and the electric potential V satisfy Laplace's equation. Therefore if an electrical analog of a fluid problem is set up such that the boundary conditions for V are exactly analogous to those for φ, then the distribution of V in the conductor will be exactly the same as the distribution of φ in the

corresponding fluid problem.

The analog may now be written

$$\varphi \equiv V$$

In this study, we are primarily interested in the distribution of the pressure p along the boundary of the flow. We can just as well study the distribution of the velocity, $\bar{v} = \nabla\varphi$, along this boundary and get p by Bernouilli's equation.

By the electrical analog stated, it is equivalent to study the distribution of the gradient of the electrical potential V along the similar boundary of the electrical analog model.

Because Ohm's Law is valid for any isotropic conductor, ∇V is proportional to ∇R, R being the resistance of the conductor. Hence the investigation proposed may be done by resistance measurements along the boundary of the electrical analog model.

III. ELECTRICAL CONSIDERATIONS

For convenience, it was decided to use an electrolyte as conductor. The electrolyte bath was connected into a Wheatstone bridge for making resistance measurements.

1. Introduction of Alternating Current

Unfortunately, it is not possible to use direct current to measure the resistance since electrolysis will occur and change the concentration of the solution and the nature of the electrodes. These difficulties can be minimized by the use of alternating current but this fact greatly increases the difficulties of measuring the resistance.

2. Mathematical Theory of the A.C. Wheatstone Bridge (Ref. 3)

The conditions of equilibrium will be reviewed briefly in order to justify the care taken in the construction of the electrical apparatus and explain some of the troubles encountered.

The bridge is illustrated schematically in Fig. 1.

The condition of balance is that the voltage across the detector be zero. This will occur when

$$\frac{Z_1}{Z_2} = \frac{Z_3}{Z_4}$$

where Z_i is a complex impedance.

In complex notations

$$\frac{R_1 + iX_1}{R_2 + iX_2} = \frac{R_3 + iX_3}{R_4 + iX_4}$$

hence $\frac{R_1}{R_2} = \frac{R_3}{R_4}$ is true only if both the equations

$$\frac{X_1}{R_1} = \frac{X_2}{R_2} \quad \text{and} \quad \frac{X_3}{R_3} = \frac{X_4}{R_4}$$

are satisfied. The best way to satisfy these conditions would be to design a bridge without reactance at all; practically this is impossible when the electrolytic tank forms the two legs of the bridge. Therefore a condenser must be inserted into the bridge to balance any capacitance effect.

3. Description of the Circuit

The general circuit arrangement employed is shown in Fig. 1. The electrolyte bath constitutes legs 3 and 4 of the bridge and variable resistances form legs 1 and 2.

Constant Voltage Transformer

Due to the high input amplification of the oscilloscope, it was found necessary to place a constant voltage transformer ahead of the bridge circuit to reduce transient and surge voltages always present in the power line.

Power Source - Introduction of an Oscillator

In making conductance measurements, it is essential to use a pure sine wave alternating current in order that no harmonics will be present when the fundamental has been balanced out. The presence of harmonics in the input of the bridge may obscure the fundamental balance.

Most of the tests have been made at 1000 c.p.s., which is the frequency generally used for the measurements of conductance in chemistry. Small changes of frequency are unimportant; however, it must be kept in mind that since the bath does not have ideal dielectric properties the bridge balance is slightly dependent upon the frequency.

Shielded Transformer

A shielded transformer is necessary to isolate the bridge from the generator and to reduce the effect of capacitance of the external circuit to ground. To achieve satisfactory accuracy, this must be a specially designed transformer for A.C. bridges such as General Radio 578-A.

Variable Resistances

Accurate resistance boxes were used to balance the bridge. The manufacturer's specifications show that these resistances are adjusted to within 0.1 per cent of the stated value and that there are no serious frequency errors below 50 KC. The total resistance of each box is 11,110 ohms.

Use of the Oscilloscope as Null Detector (Ref. 4)

The output of the bridge is applied through a 40 db.amplifier to the vertical deflecting plates of a cathode ray oscilloscope whose horizontal deflecting plates are connected to the oscillator. A tilted ellipse appears on the screen unless both capacitance and resistance are adjusted to balance; in this case the tilted ellipse becomes a horizontal straight line.

The preamplifier was needed to increase the sensitivity since only 1.5 volts were put across the bridge.

This method permits independent adjustment of the resistance and reactance which is a great advantage over detection by a vacuum voltmeter or a telephone. And moreover disturbances such as A.C. hum, stray pickup, tube noise or harmonics generated by the oscillator are easily detected. This null indicator cannot be injured by overloading.

Shielding and Grounding

The midpoint D of the bridge was grounded.

The leads between bridge and amplifier were shielded and the shields carefully grounded. The other leads were not shielded to avoid unnecessary capacitance to ground. The resistance boxes were shielded and grounded.

To reduce external pickups and capacitances, the exploring probes were cut short outside the boundary.

With this set up, the readings of the bridge were practically independent of its surroundings and position of observer. The 60 cycle pickup from the surrounding lines never gave serious trouble, even for readings at the middle of the bridge.

It must be pointed out here that for high precision work, grounding the bridge at its midpoint is inadmissible but an adaptation of the Wagner ground must be used (Ref. 3).

Electrolyte Considerations

For convenience, it was decided to use a weak solution of copper sulfate in distilled water together with copper electrodes and exploring probes.

Most of the runs were made with a solution containing about 4 grams per liter. A few drops of sulfuric acid were added to the stock solution to reduce the oxide deposit on the terminal plates.

Corrosion at the surface of the current carrying electrodes, setting up an electrolytic capacitance, was made sufficiently small by raising the operating frequency to 1000 c.p.s. as already explained, and by keeping the current density low. A high frequency also minimized

the non-linear conduction due to polarization of the electrodes surface.

A check was made of the current density on the electrodes and it was found that in all cases it was less than 0.05 mA/cm.^{2}. The current in the bath was approximately 1 mA. It is believed that using a current at least five times greater would have made the electrical measurements easier without serious danger of corrosion of the electrodes' surface.

The molal conductance* of the solution used was about $\Lambda = 63$.

For an average model this gives a total resistance between terminal plates of a few thousand ohms.

The exploring probes do not carry any appreciable current and none of the above trouble arises here.

*The molal conductance is defined by $\Lambda = 10^6 \kappa / C$ where κ is the specific conductance in ohm^{-1} cm.$^{-1}$ and C the concentration in milli-formula-weights per one liter of solution.

IV. THE MODEL

1. Constructional Details

The model was built on the same general plan as used at the Iowa Institute of Hydraulic Research (Ref. 2).

Only a segment of the axially symmetrical analog conductor was formed by filling with electrolyte the space between a tilted glass base, the insulator boundaries and the terminal copper plates as shown in Fig. 2. The center line of this conductor is the intersection of the electrolyte free surface with the glass.

The constructional details of the tank together with the mounting of the electrodes and exploring probes are shown in Fig. 28. It can be seen that the base of the tank consists of a 1/4 in. thick 27 x 40 in. glass plate resting on a very flat plywood baseboard which can be accurately levelled by three levelling screws.

Boundary

The boundaries consist of strips of vinylite 50 x 3 in. and 0.04 in. thick maintained perpendicular to the glass base by supports spaced 8 cm. apart. This of course is only an approximation for the boundary of a surface of revolution.

It would have been preferable to use polystyrene which is an insulating material having a high resistance to leakage currents and a very low water absorption; however this material was not available at the time.

Probes

To record precisely the potential at any point of the electrolyte,

the probes must be of small diameter. They were made of copper wire 0.38 mm. diameter and were inserted in holes drilled perpendicular to the boundary and uniformly spaced.

The boundary was checked on a comparator to see that the cross section of the probes was circular and the spacing between successive probes was recorded. It was found, for example, that for one of the strips used, the average distance between probes was d = 20.065 mm. with a standard deviation δ = 0.21 mm. (based on 60 probes). Since the deviation in spacing was so small, it was decided to use a constant value for d in the calculations of the velocity from the measurements of the potential at two consecutive probes.

Current Carrying Electrodes

These electrodes were made of a strip of copper 3 in. wide, 1/32 in. thick glued on polystyrene for rigidity. In order to follow a potential line these electrodes could be bent with a wood template when necessary.

2. Experimental Technique

No particular technique is involved, but great care is necessary to build the model, level it accurately, etc.

Setting the Plastic Boundaries

A precise drawing of the boundary curve to be tested was made and inserted between the glass and wood support so that the center line of the model would be parallel to a line connecting the centers of two of the levelling screws.

The plastic boundaries are then fitted in place and glued to the glass with a mixture of beeswax and rosin. This wax sticks perfectly

if the glass has been well cleaned with toluene or acetone and boiling water. No templates were used; however checks have shown that it is possible to set the plastic strip well within 1/2 mm. of the drawing.

The terminal electrodes were placed in the same manner.

Center Line Limitation

To be sure that the electrolyte does not rise by capillarity above the center line, a small paraffine wall was built along the center line.

Boundary Seal

White shellac applied with a small brush was found to make a very good seal between the boundaries and the glass. Shellac is a good insulator and does not attack vinylite (or polystyrene); it can be applied in a thin layer, dries quickly, and can be removed easily with methyl alcohol.

Levelling the Model

The center line was placed horizontal and a slope of about 5 to 8/100 was given to the model base. This angle is arbitrary so long as it is small; as already said, a limitation to it is the fact that the cross section of the boundary is not a circle but is a short straight line perpendicular to the glass base.

The levelling was done with considerable precision using an accurate level.

It is important to set up the center line exactly horizontal, because if it is not a flow believed to be parallel, for example, would actually be conical.

Filling the Model

The model was carefully washed with detergent before being

filled; this procedure reduces slightly the surface tension.

In order to fill the model exactly to the center line level, it was necessary to use a special point gage (see Fig. 3). The use of this gage made it possible to level the water within $\pm$ 0.0038 cm. of the level of the center line. This insured good reproductibility of a run.

It must be pointed out that the actual axis of the flow corresponds to the intersection of the free surface of the electrolyte with the glass base.

Miscellaneous Remarks

It was necessary to cover the model when measurements were taken since the slightest motion of the air created capillary waves which took a long time to damp out and made readings difficult to obtain.

The electrolyte was never left in the bath longer than necessary for a run to avoid deposit of copper sulfate crystals

The electrodes were cleaned often with sandpaper to reduce the capacitance.

Calculations

When the bridge is balanced for probe i

$$\frac{(R_4)_i}{R} = \frac{(R_2)_i}{(R_1+R_2)_i}$$

where $(R_1)_i$ and $(R_2)_i$ the resistances balancing the bridge, $(R)_i$; the resistance between probe i and one of the two terminal plates, and R the total resistance of the bath.

The spacing between two probes being considered as unity, the difference

$$\Delta R = (R_4)_{i+1} - (R_4)_i$$

is an approximation for the gradient ∇R considered at the mid-point between probes i and $(i+1)$.

V. CHECKING THE PERFORMANCE OF THE TANK

1. Preliminary Checks

Since the analog requires that the boundaries be perfect insulators, that is, $\frac{\partial \varphi}{\partial n} = 0$ the model was tested with a Weston Insulator Tester and it was found that the resistance between any two points, that is, two probes, electrodes, or seal, was higher than 10,000 M when dry.

To find out if the electrical apparatus was reliable the bath was replaced by known resistances and capacitances lumped to as to duplicate the condition of a run. In measuring these known resistances with the bridge, it was found that the relative error in the resistance readings was always less than 0.3 per cent.

The easiest method of checking the overall performance of the tank is to set up a simple flow example for which the theoretical solution is known. Two such checks were made, namely flow in a cone and in a hyperbolic type boundary.

2. Accuracy Determination

Conical Flow

The potential φ for a source flow (or sink) is given by

$$\varphi = -\frac{Q}{4\pi\rho}$$

where ρ is the radius from the origin and Q the source strength. The velocity along a line passing through the origin O is

$$v = \frac{\partial \varphi}{\partial \rho} = \frac{Q}{4\pi}\,\frac{1}{\rho^2} \quad ,$$

or in dimensionless form

$$\frac{v}{v_o} = \left(\frac{\rho_o}{\rho}\right)^2$$

where ρ_o is a reference radius.

The model built represented the flow in a cone having for vertex angle 24^o (see Fig. 4).

The experimental points have been plotted together with the theoretical curve on Fig. 5.

An analysis of the results shows that the overall accuracy is better than 1 per cent, the greatest discrepancy being, of course, for the smallest radius.

The results of two different runs for about 15 points are shown in Table I. It appears that by working carefully it is possible to reproduce quite well a set of data.

Hyperbolic Flow

This is another case where the mathematical solution can be easily derived. A homogeneous polynomial of the type

$$\varphi = k \left(\frac{r^2}{2} - z^2 \right)$$

will satisfy $\nabla^2 \varphi = 0$.

Using the expressions for the radial and axial velocities v_r and v_z, that is,

$$v_r = \frac{1}{2\pi r} \frac{\partial \Psi}{\partial z} \qquad , \qquad v_z = - \frac{1}{2\pi r} \frac{\partial \Psi}{\partial r}$$

it is found that the corresponding stream function is

$$\Psi = 2\pi k \, r^2 z \quad .$$

The boundary has been set up for $\frac{\Psi}{2\pi k} = 20$, hence,

$$\varphi = \frac{1}{2\pi} \left(\frac{r^2}{2} - z^2 \right)$$

and the velocity gradient along this boundary is given in dimensionless form by

$$\frac{V}{V_0} = \sqrt{\frac{1600 + r^6}{1600 + r_0^6}} \cdot \left(\frac{r_0}{r}\right)^2$$

The experimental points are shown along with the computed curve on Fig. 6. Here again the experimental results are within 1 per cent of the theoretical values.

It is interesting to point out that this second run has been quite useful for the design of the curved plastic boundary. It was found that the first plastic strip made was entirely inadequate because the vertical supports cemented behind the strip were 3/16 in. thick; this caused a large bending moment to occur in the strip at these points which made it impossible to bend the boundary along a smooth curve.

3. Discussion of the Accuracy - Sensitivity

The precision with which the bridge can be balanced depends primarily upon the applied voltage and sensitivity of the null detector. The sensitivity is variable during a run, depending on the ratios of the arms, but in all cases it was possible to balance out the bridge to the nearest ohm out of 9000 ohms.

An overall accuracy to within 1 per cent has been obtained in the check runs.

It is believed that the precision with which the boundary can be put in place is the limiting factor; since this precision is independent of the size of the model, the accuracy would have been better if larger models had been built (the glass base used was 40 x 27 in.). However in larger models, thermogradients and settling of the solution might

give troubles.

In the subsequent runs where less care has been taken in setting the boundary, the overall accuracy was estimated to be within 2 per cent.

It should be pointed out here that there has always been a slight shift in zero of the potential during a run. This has been tentatively attributed to the changes in meniscus shape along the current carrying electrodes and to evaporation of the electrolyte during a run. This shift has no effect on the velocity distribution, that is, derivative of potential as long as it is reasonably small.

VI. TEST OF A RADIAL FLOW IMPELLER CHANNEL

As an application of the electrical analog, it was decided to study the meridional velocity distribution in a typical well designed commercial radial flow impeller channel before making a systematic survey of the transition curves. The purpose of this run was to give a better idea of the magnitude and sharpness of the pressure drop to be expected and to decide upon the parameters to be varied in the subsequent experiments.

The terminal plates were put about 2.5r and 1.2b from the curved part, so as not to disturb the flow pattern.

The experimental velocity along the front and back shrouds is plotted in dimensionless form in Fig. 8.

One notices, as expected, a sharp increase in meridional velocity near the point of tangency D of the front shroud and the approach section; the maximum velocity is 1.27 greater than the average axial flow velocity.

It is interesting to point out that the velocity starts increasing about one radius upstream of D.

VII. SYSTEMATIC STUDY

In order to facilitate a systematic study of flows in impeller channels it has been decided to use, as front and back shroud curves, a family of simple curves depending only on a few parameters.

1. Choice of Boundary Curves

A survey of some radial flow impellers showed that the front shroud, often made out of circular arcs, can be well approximated by a quarter of an ellipse having its semi-axes parallel to the axial and radial directions.

Since the back shroud was more difficult to fit to a simple curve, a separate study was made to find out the effect of the back shroud profile on the velocity distribution along the front shroud, which is our main concern. For this study four runs were made using ellipses defined by Fig. 10 as back shroud curves. The ratio of the semi-axes was the only variable, namely

$$\frac{a_2'}{a_1'} = 0 \; ; \; 0.492 \; ; \; 0.708 \; ; \; 1.0$$

The other characteristic lengths were chosen similar to those of the radial impeller tested (see Part VI), that is,

$$\frac{a_1}{a_2} = 1.1 \qquad \frac{r_2}{r_1} = 1.9 \qquad \frac{A_1}{A_2} = \frac{1}{2}$$

The results of this investigation are shown in Figs. 11 to 14. It can be seen that, except for the case $\frac{a_2'}{a_1'} = 1.0$, the maximum velocity on the front shroud is very little affected by the back shroud curve. The ratio $\left(\frac{v}{v_0}\right)_{max.}$ varies between 1.22 to 1.24, v_0 being the velocity of the axial flow.

The back shroud curve affects mostly the sharpness of the peak of the velocity curve along the front shroud profile. For large values of $\frac{a_1'}{a_2'}$, the velocity distribution along the back shroud indicates a stagnation point at E.

For simplicity, it was decided to use as the back shroud profile a quarter of an ellipse having the same center and the same axes as the front shroud ellipse.

Refer to Fig. 3 for the definition of the characteristic lengths.

2. Outline of the Proposed Study

It was then possible to make a rather systematic investigation of the transition flows.

Three sets of four runs were made. The ratio $\frac{r_2}{r_1} = 1.9$ was kept constant for all runs. Each set corresponding to a given inlet to outlet area ratio and each run to a given curvature of the front shroud.

Three different area ratios were considered; namely,

$$\frac{A_1}{A_2} = \frac{1}{2} \; ; \; \frac{3}{4} \; ; \; 1 \; .$$

For a given area ratio, the four curvatures of the inside shroud were given by

$$\frac{a_1}{a_2} = 1.0 \; ; \; 1.1 \; ; \; 1.3 \; ; \; 1.6 \; .$$

The back shroud ellipse is defined by $\frac{a_1'}{a_2'}$ in each case from the knowledge of

$$a_1' = r_2$$

$$a_2' = a_2 + \frac{r_1}{2}\left(\frac{A_1}{A_2}\right)\left(\frac{r_1}{r_2}\right) \; .$$

Table II shows the characteristic lengths for each run.

VIII. ANALYSIS OF THE RESULTS. CONCLUSIONS

The results of the investigation have been plotted in dimensionless form in Figs. 16 to 27.

The coordinates used are:

Ordinate $\frac{v}{v_0}$, ratio of the velocity at any point on the boundary to the average axial flow velocity.

Abscis $\frac{s}{r_1}$, ratio of the distance along the boundary to the radius of the axial flow section.

The origins for s are the points of tangency of the front and back ellipses with the radial direction; these points are called B and A respectively.

In addition on every figure, the point of tangency of the front ellipse with the axial direction is marked D.

1. Velocity Distribution Along the Front Shroud

A brief inspection of Figs. 16 to 27 shows that the meridional velocity between B and D is not a monotonic increasing function as one would like, but instead in all cases there is a peak in the meridional velocity just before the point of tangency D; also in all cases the effect of the curvature can be seen for about one radius after D.

Fig. 15 shows how the maximum relative velocity $\frac{v}{v_0}$ is dependent on the geometrical ratios $\frac{A_1}{A_2}$ and $\frac{a_1}{a_2}$ defining the transition curve. This diagram can be used to get an estimate of the meridional velocity to be expected along the front shroud of a radial flow impeller channel.

For example, the impeller shown in Fig. 7 can be characterized

by

$$\frac{A_1}{A_2} = 0.57 \qquad \frac{a_1}{a_2} = 1.2$$

using Fig. 15 we get approximately 1.28 as a maximum relative meridional velocity on the front shroud. A separate study of this impeller channel (Part VI) gave $\frac{V}{V_0}_{max} = 1.27$.

2. Velocity Distribution Along the Back Shroud

The velocity distribution along the back shroud is plotted for each run in the same dimensionless form as the velocity along the front shroud.

It can be noticed that the average velocity at radius r_2 is in the ratio $\frac{A_1}{A_2}$ to the velocity of the axial flow as it should be.

For $r > r_2$ the front and back shroud velocities approach each other and become very quickly equal. This confirms that the end plate was far enough from the impeller end in a region of uniform radial flow. For large r the velocity distribution is that of a two-dimensional source (or sink).

3. Conclusions

The meridional velocity distribution along twelve different transition curves has been investigated. These transitions include most of the radial-flow turbomachinery and by extension mixed-flow turbomachinery.

From a knowledge of the meridional velocity along the boundaries, the velocity at any point in the channel can be obtained by successive approximation, but these computations were not done here. However,

it would be of interest for pump designers to know better the velocity distribution across the channel breadth. In design computations this velocity is generally assumed to vary monotonically from one end of the impeller to the other and to be constant over the passage breadth. Inspection of the velocity plots shows that this assumption is considerably in error, so that the velocity variation along meridian streamlines should be taken into account for blade design.

Whether or not these results are much influenced by real fluid effects and by the action of the blades is not known. In order to discuss this point it would be necessary to make further investigations, including experimental work.

REFERENCES

1. Wislicenus, G. F.: Fluid Mechanics of Turbomachinery. McGraw-Hill (1947).

2. Hassan, M. M.: Use of the Three-Dimensional Electrical Analog in the Design of Conduit Contractions. Ph.D Thesis, State University of Iowa, Iowa City.

3. Jones, Grinnel and Joseph, Roswell Colt: The Measurement of the Conductance of Electrolytes. I. An Experimental and Theoretical Study of Principles of Design of the Wheatstone Bridge for the Use with Alternating Currents and an Improved Form of Direct Reading Alternating Current Bridge. J. Am. Chem. Soc., Vol. 50, 1049 (1928).

4. Jones, Grinnel, Mysels, Karol J. and Juda, Walter: The Measurement of the Conductance of Electrolytes. IX. The Use of the Cathode-Ray Oscillograph as Detector. J. Am. Chem. Soc., Vol. 62, 2919 (1940).

Electrode No.	Run 1	Run 2	Error $\frac{1-2}{1}$
1	0.548	0.547	0.0018
2	0.568	0.571	0.0053
3	0.603	0.600	0.0050
4	0.623	0.621	0.0032
5	0.657	0.656	0.0015
6	0.691	0.689	0.0029
7	0.723	0.720	0.0041
8	0.754	0.751	0.0040
9	0.800	0.798	0.0025
10	0.846	0.839	0.0083
11	0.885	0.885	0.0000
12	0.937	0.934	0.0032
13	1.000	1.000	0.0000
14	1.056	1.049	0.0066
15	1.119	1.112	0.0059
16	1.202	1.200	0.0017
17	1.261	1.264	0.0024

CONICAL FLOW

COMPARISON OF TWO RUNS

TABLE I

Run	$\frac{r_2}{r_1}$	$\frac{A_1}{A_2}$	$\frac{a_1}{a_2}$
B_1	1.9	1/1	1.0
B_2	1.9	1/1	1.1
B_3	1.9	1/1	1.3
B_4	1.9	1/1	1.6
C_1	1.9	3/4	1.0
C_2	1.9	3/4	1.1
C_3	1.9	3/4	1.3
C_4	1.9	3/4	1.6
D_1	1.9	1/2	1.0
D_2	1.9	1/2	1.1
D_3	1.9	1/2	1.3
D_4	1.9	1/2	1.6

RATIOS DEFINING THE TRANSITION CURVES

TABLE II

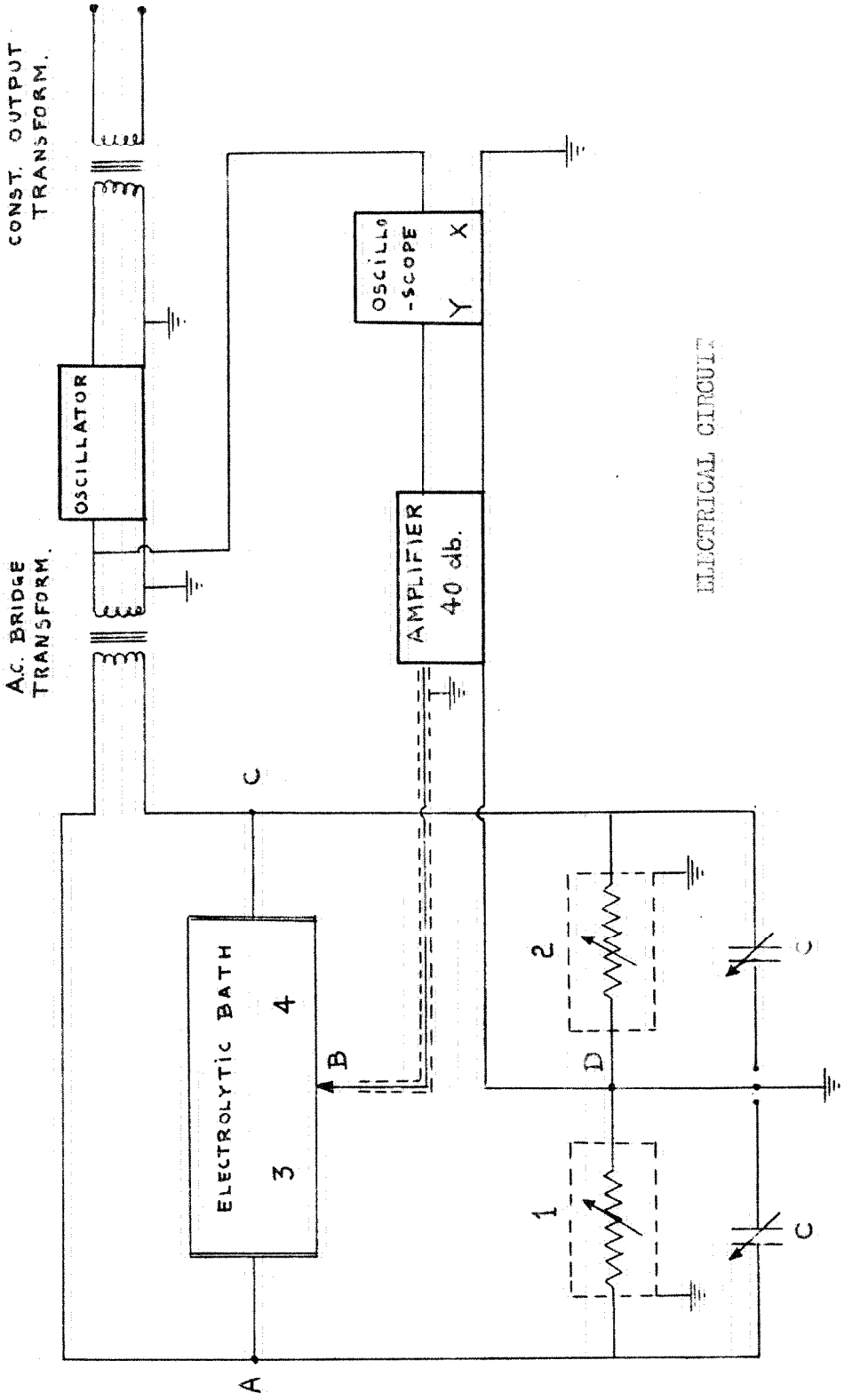
CONST. OUTPUT TRANSFORM.
OSCILLATOR
A.C. BRIDGE TRANSFORM.
OSCILLO -SCOPE
X
Y
AMPLIFIER 40 db.
ELECTRICAL CIRCUIT
ELECTROLYTIC BATH
3
4
A
B
C
D
1
2
C
C

Fig. 1

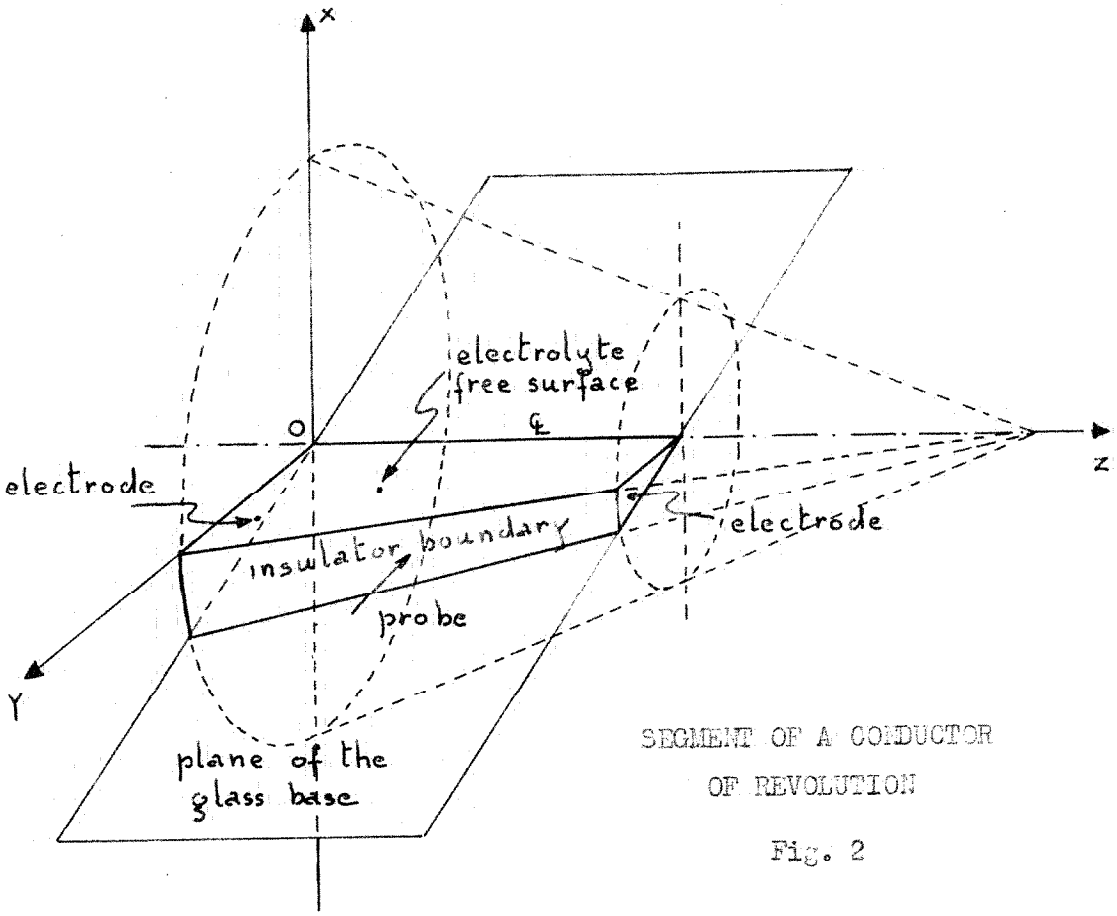

SEGMENT OF A CONDUCTOR
OF REVOLUTION

Fig. 2

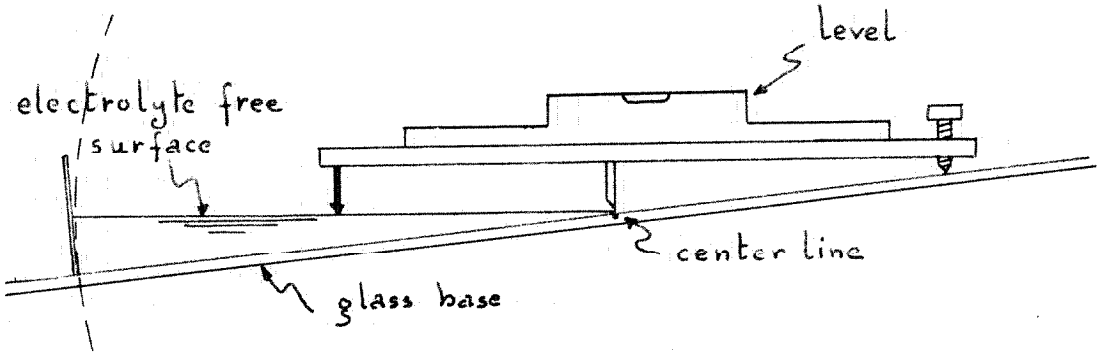

POINT GAGE

Fig. 3

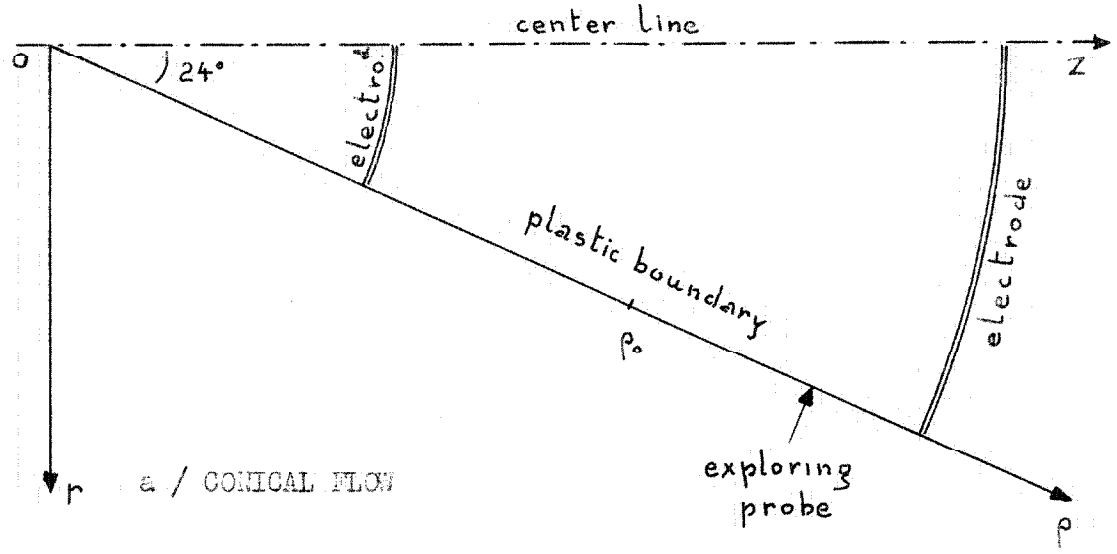

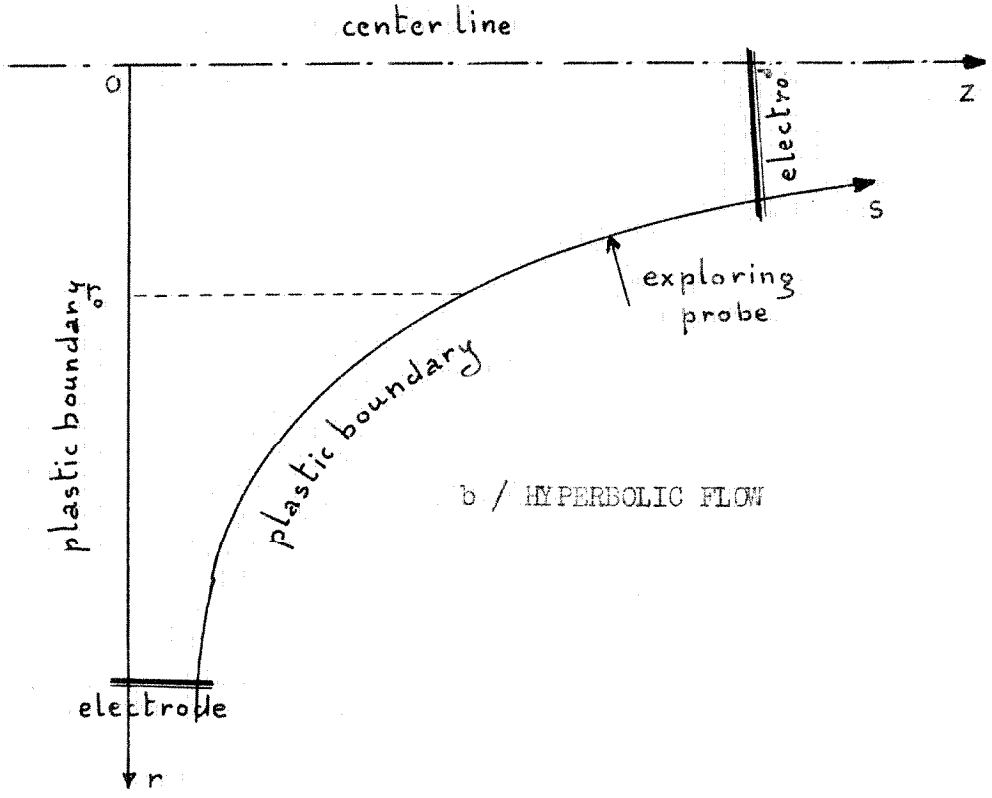

ACCURACY DETERMINATION

Fig. 4

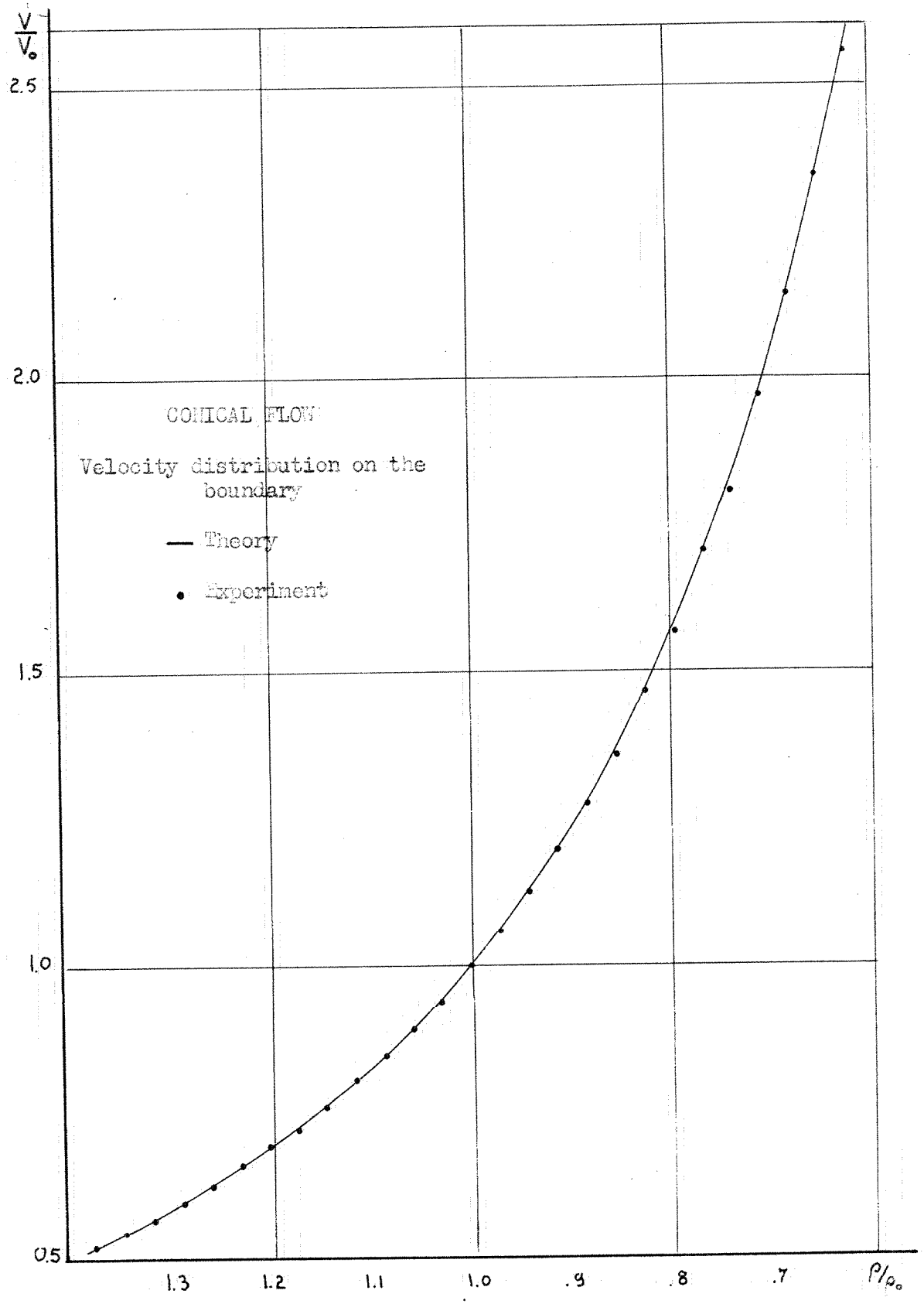
V/V₀
2.5
2.0
1.5
1.0
0.5
CONICAL FLOW
Velocity distribution on the boundary
— Theory
• Experiment
1.3
1.2
1.1
1.0
.9
.8
.7
ρ/ρ₀

Fig. 5

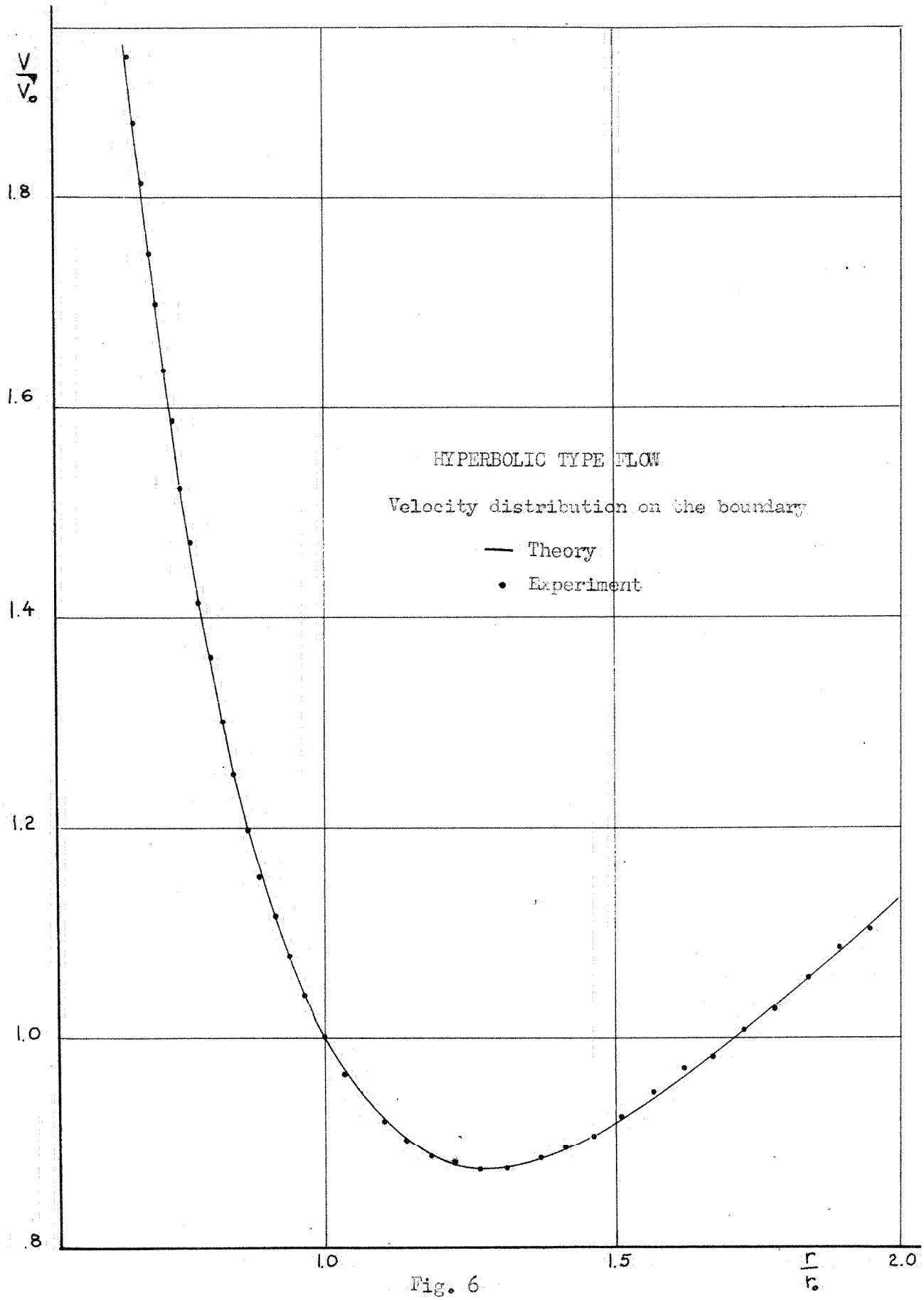
V/V₀
1.8
1.6
1.4
1.2
1.0
.8
HYPERBOLIC TYPE FLOW
Velocity distribution on the boundary
Theory
Experiment
1.0
1.5
2.0
r/r₀

Fig. 6

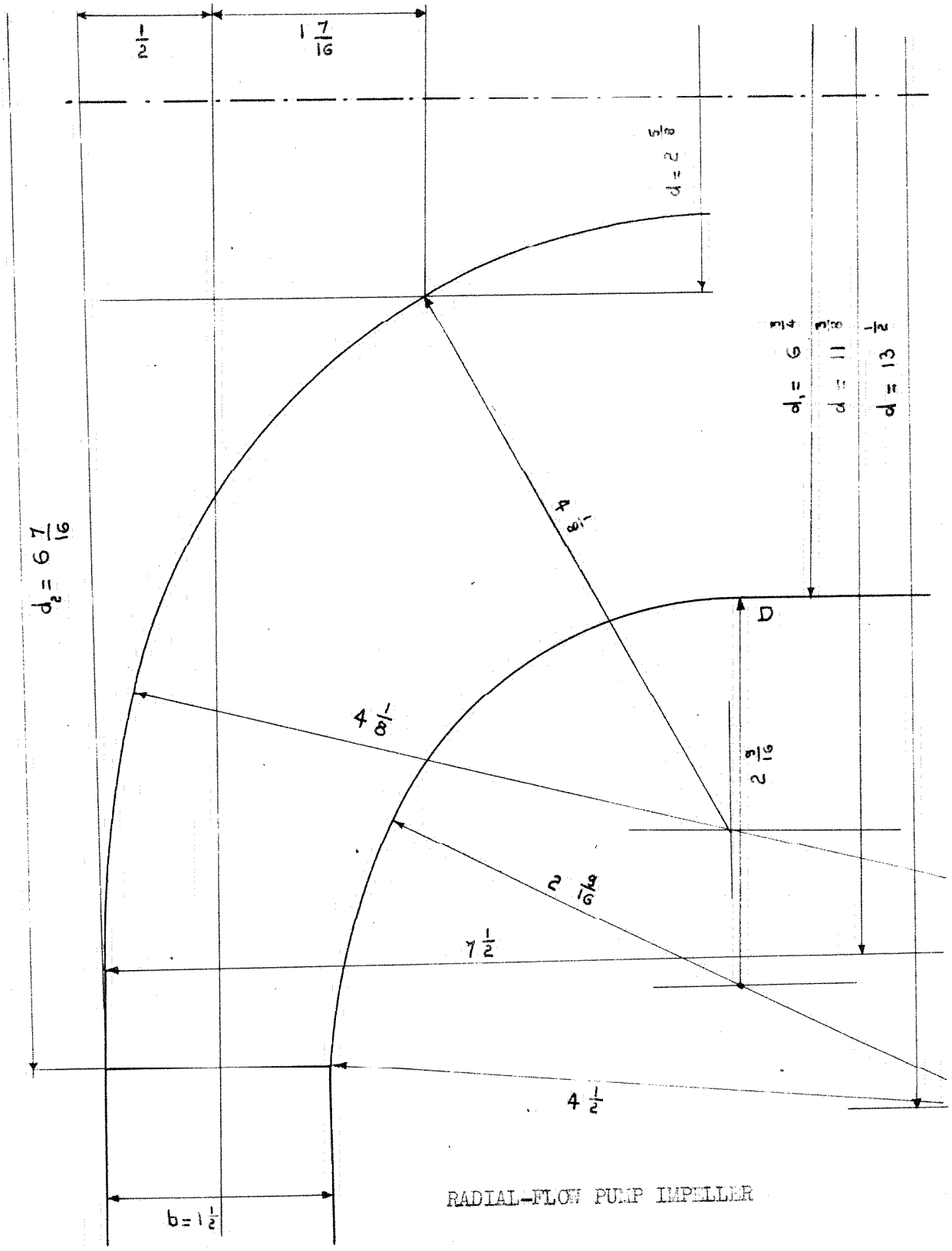

RADIAL-FLOW PUMP IMPELLER

Fig. 7

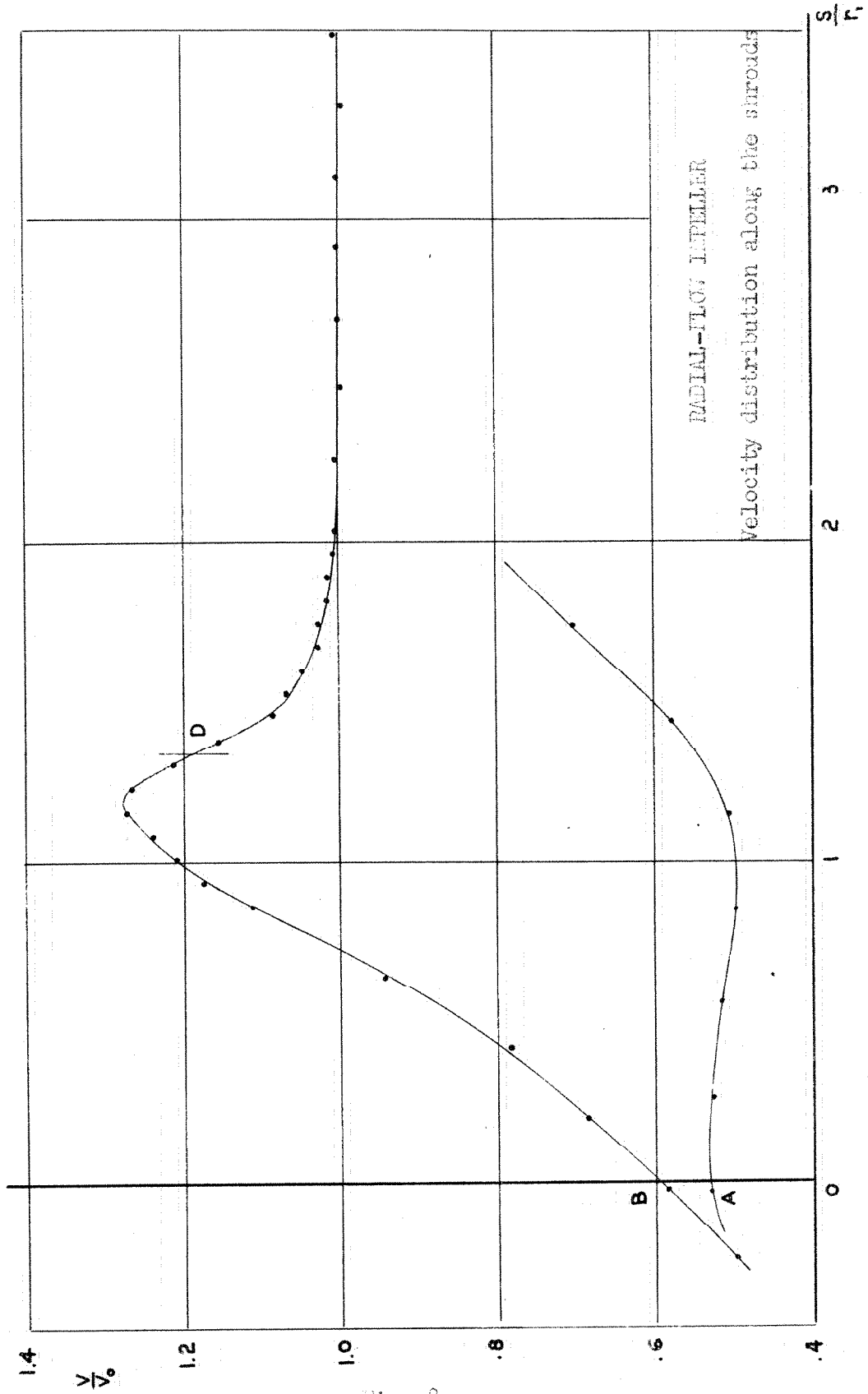
RADIAL-FLOW IMPELLER
Velocity distribution along the shroads
V/V₀
S/R
1.4
1.2
1.0
.8
.6
.4
0
1
2
3
A
B
D

Fig. 8

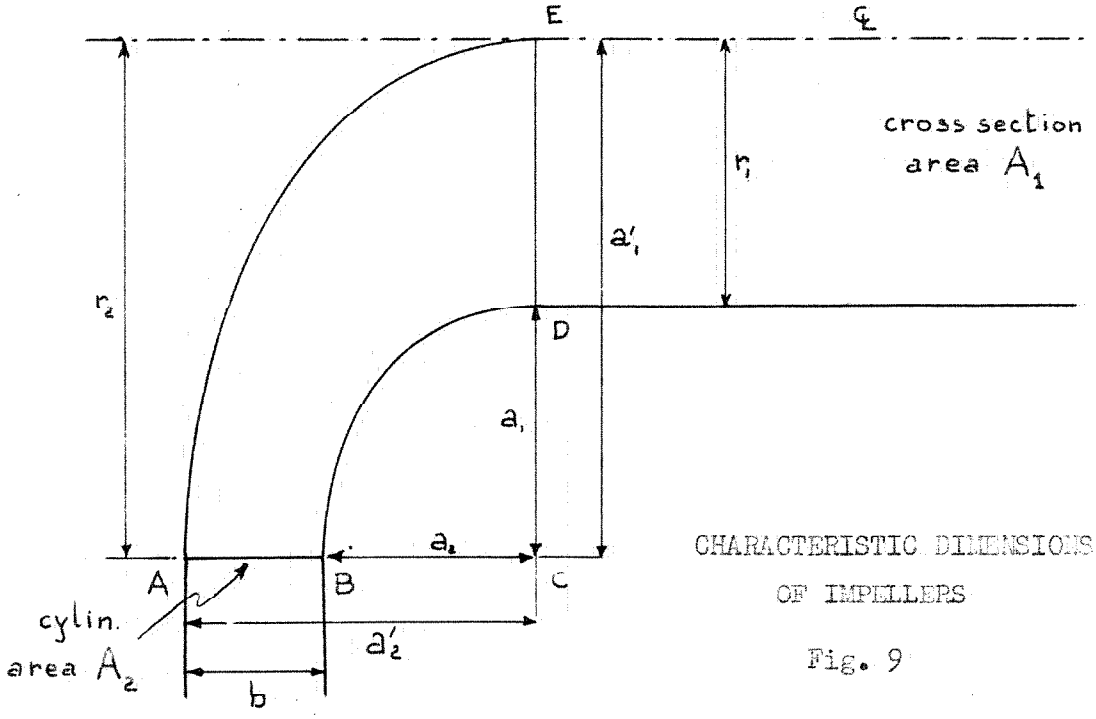

CHARACTERISTIC DIMENSIONS OF IMPELLERS

Fig. 9

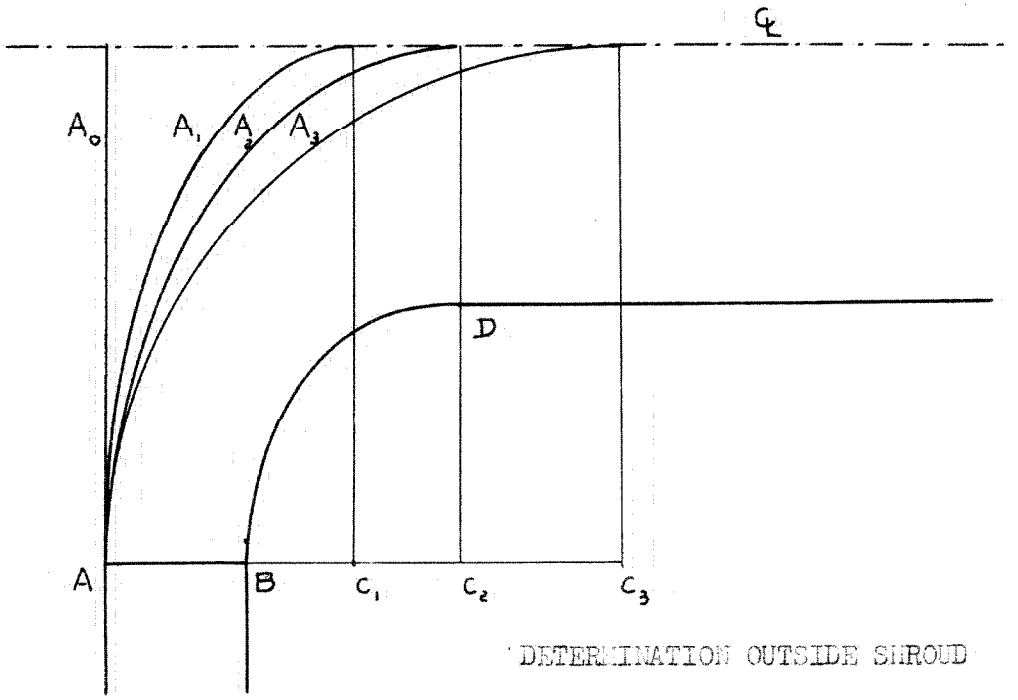

DETERMINATION OUTSIDE SHROUD

Fig. 10

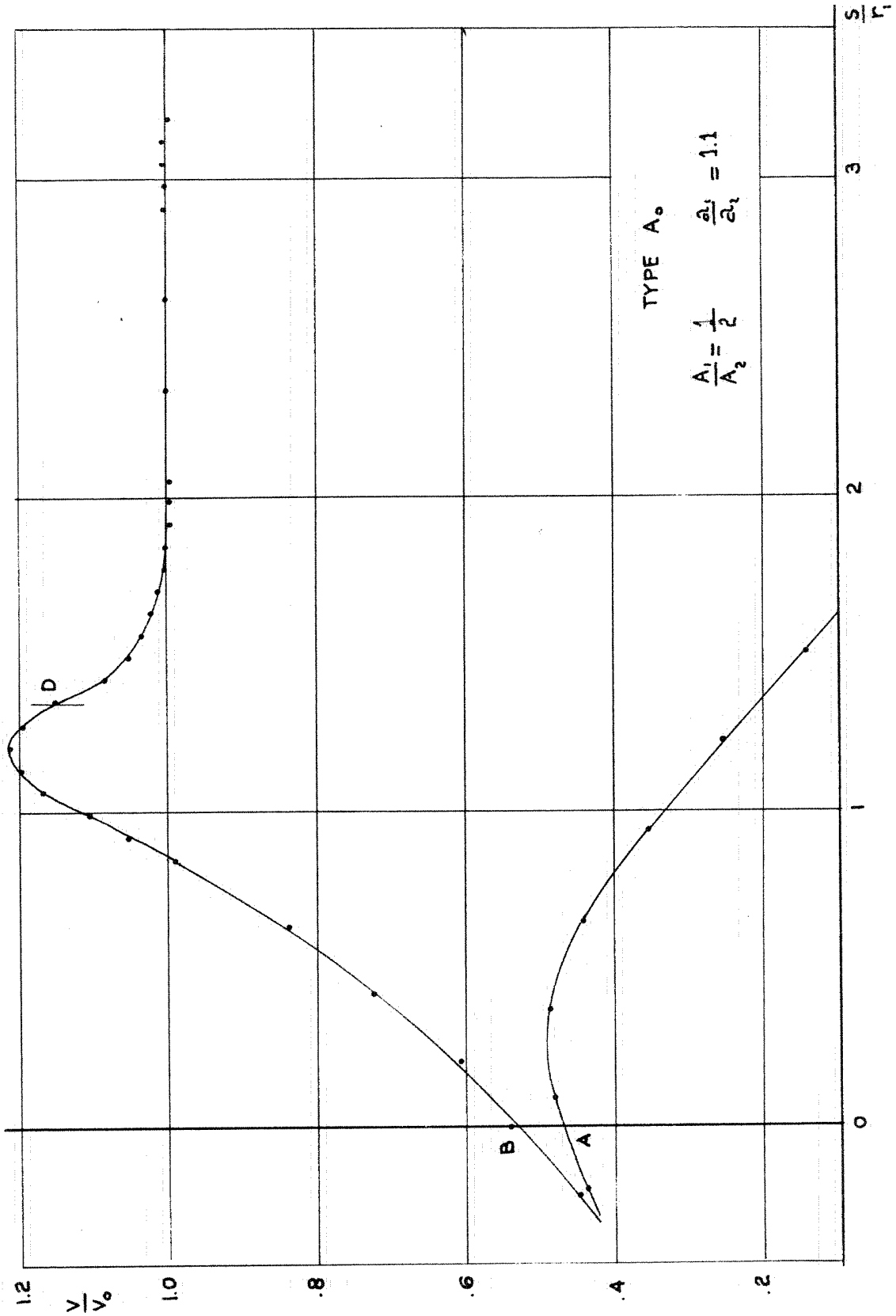

Fig. 11

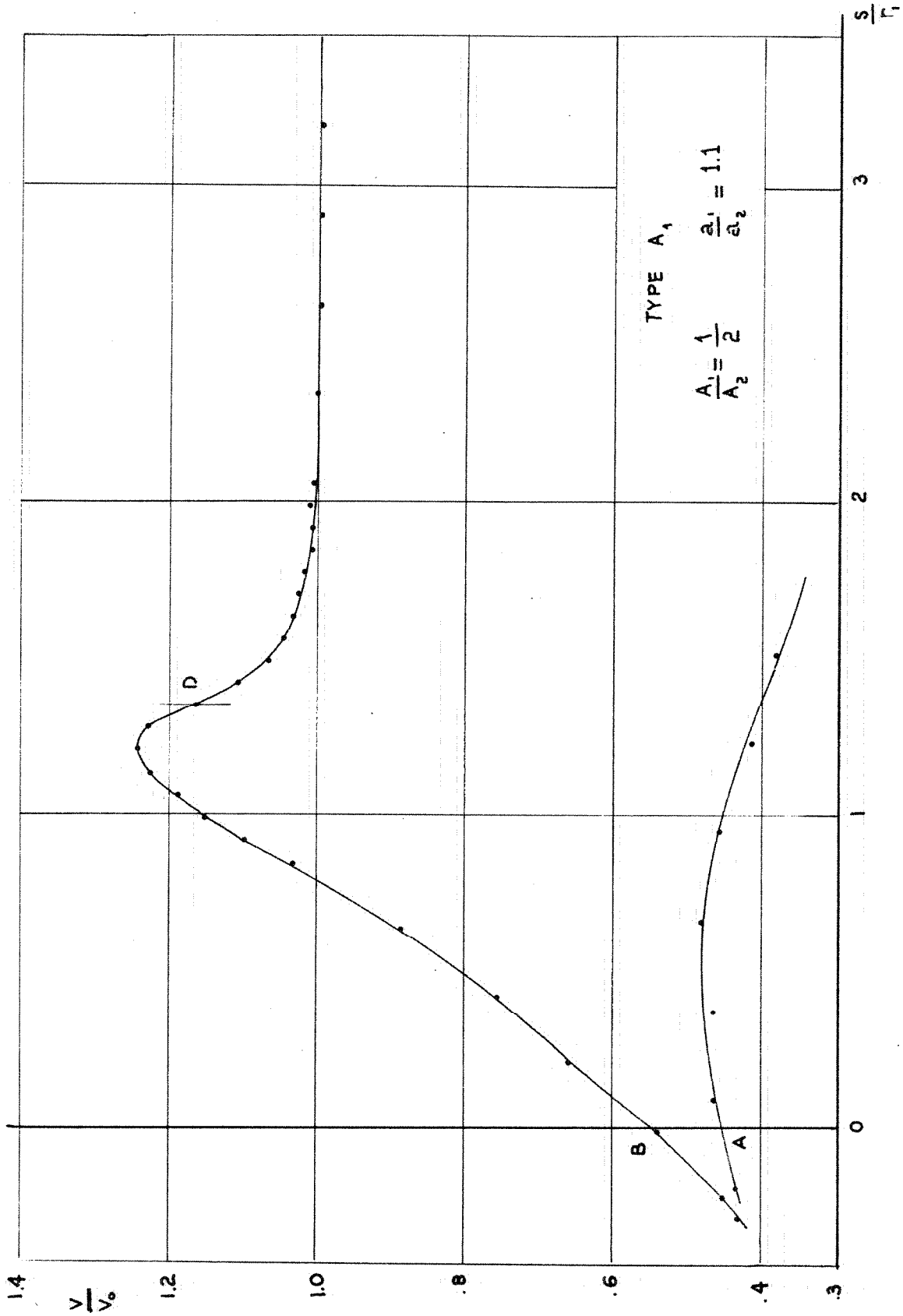

Fig. 12

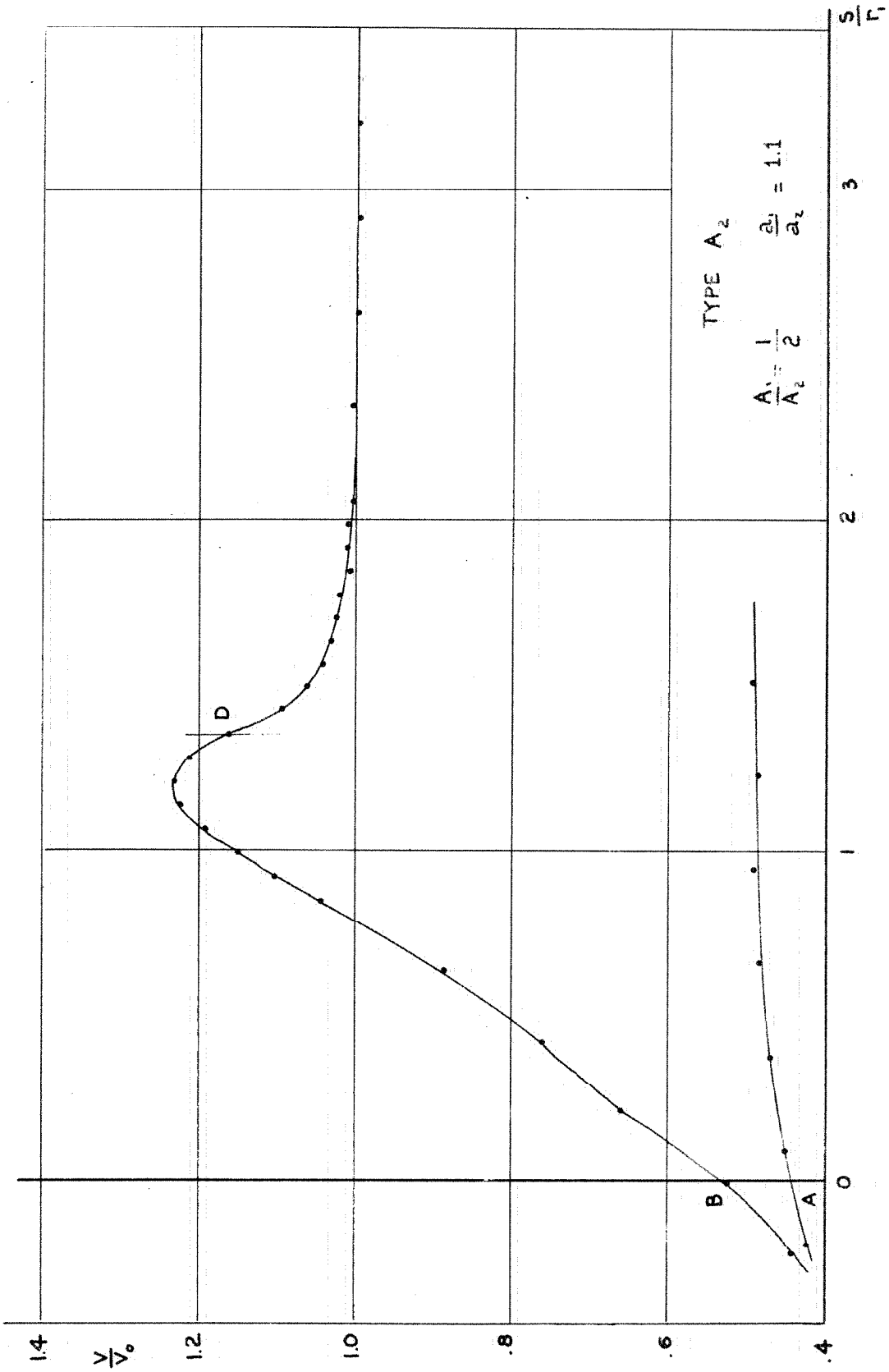

Fig. 13

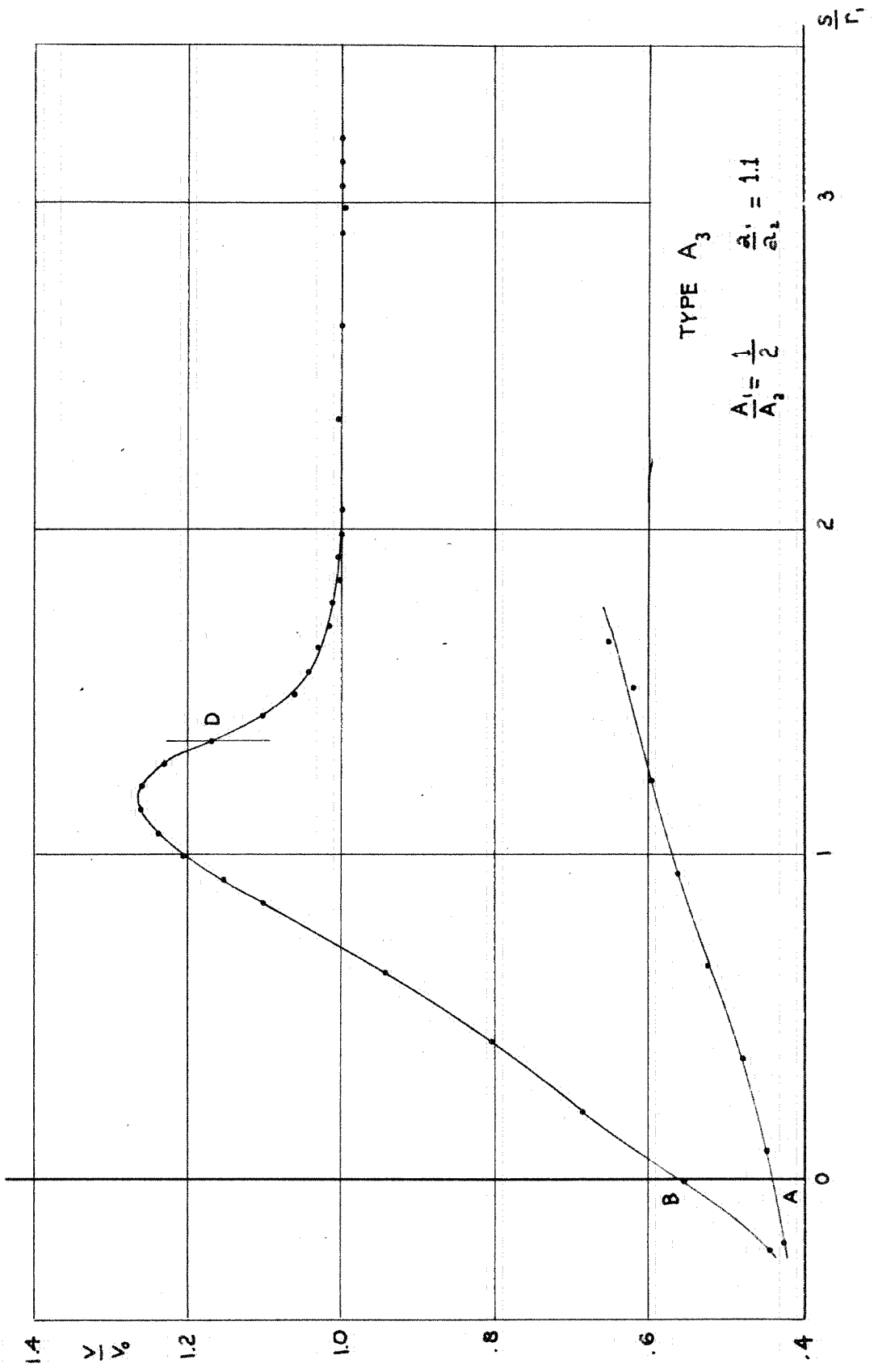
TYPE A_3
$\frac{A_1}{A_2} = \frac{1}{2}$
$\frac{a_1}{a_2} = 1.1$
D
A
B
V/V_0
1.4
1.2
1.0
.8
.6
.4
0
1
2
3
S/r_1

Fig. 14

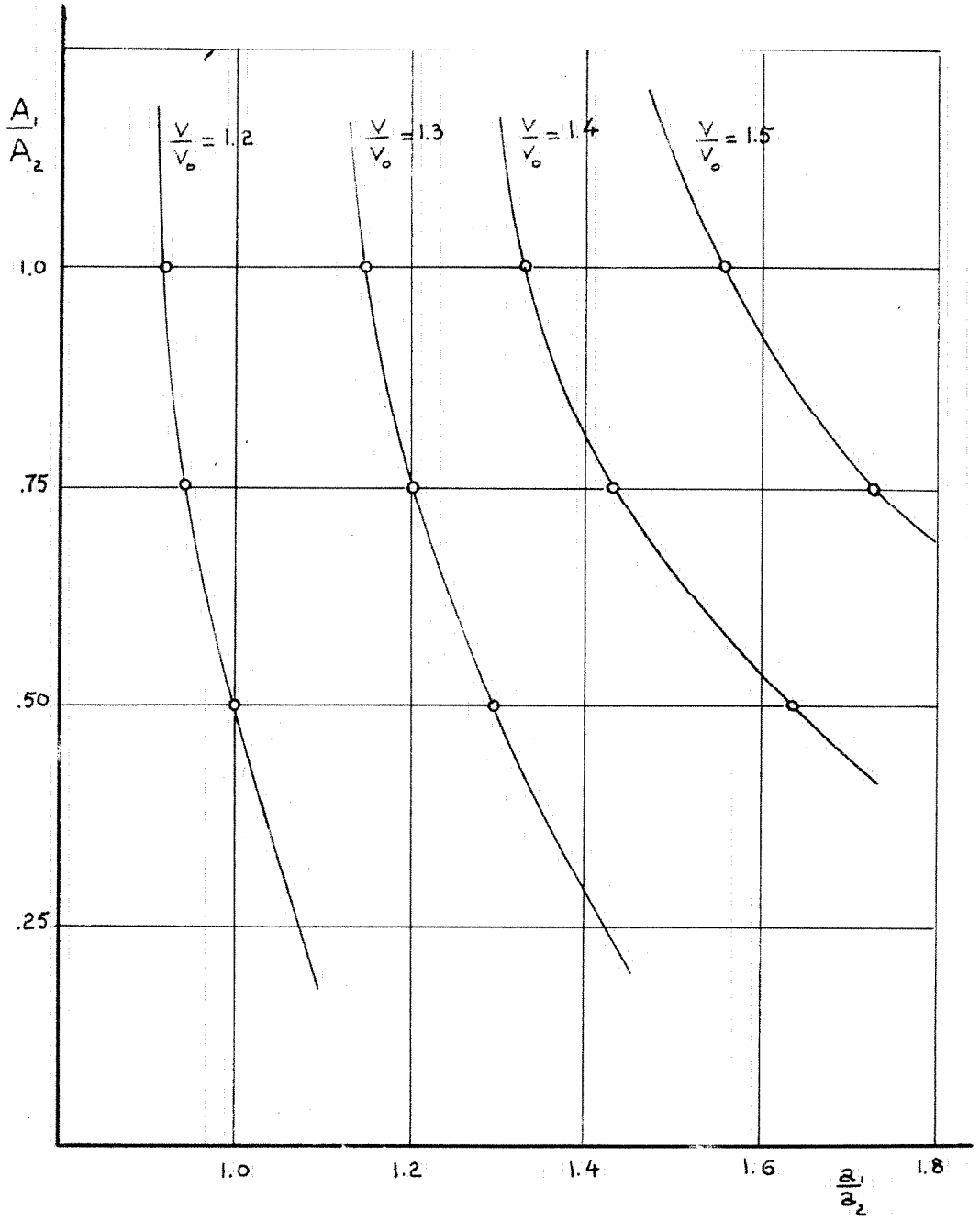

MAXIMUM MERIDIONAL VELOCITY ON THE FRONT SHROUD

Fig. 25

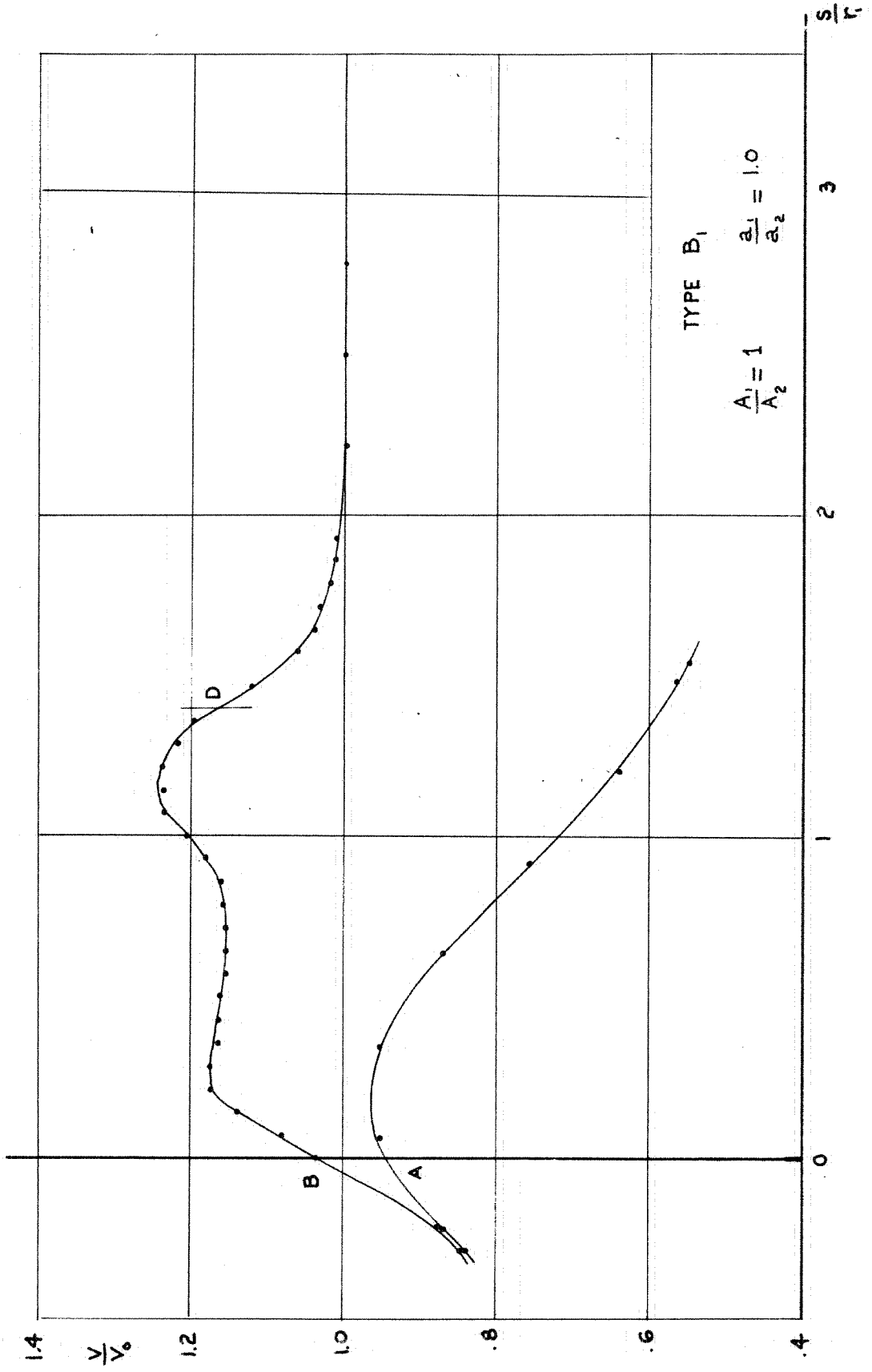

Fig. 16

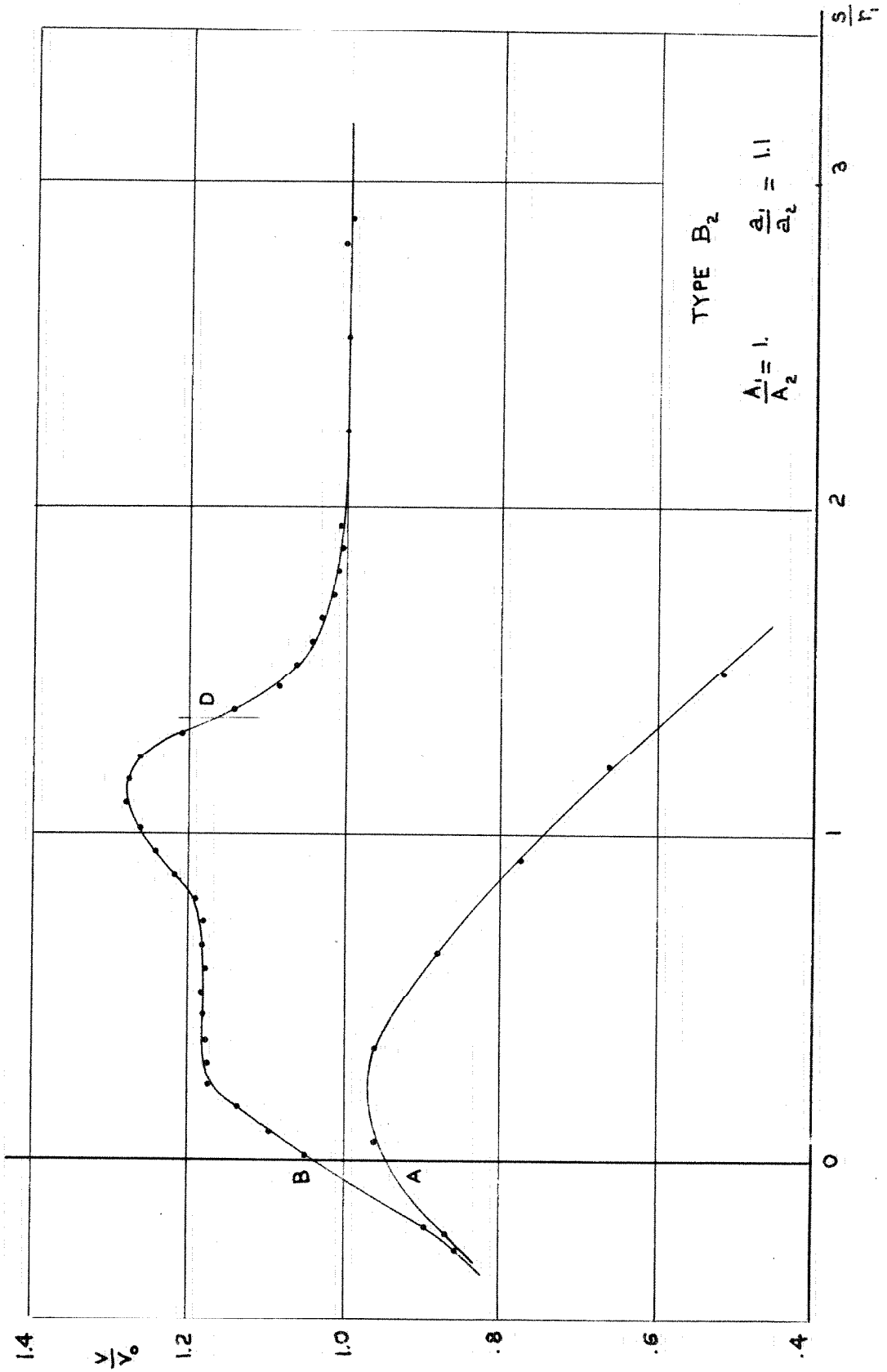
TYPE B_2
$\frac{A_1}{A_2} = 1.$
$\frac{a_1}{a_2} = 1.1$
A
B
D
$\frac{V}{V_0}$
1.4
1.2
1.0
.8
.6
.4
0
1
2
3
$\frac{S}{r_1}$

Fig. 17

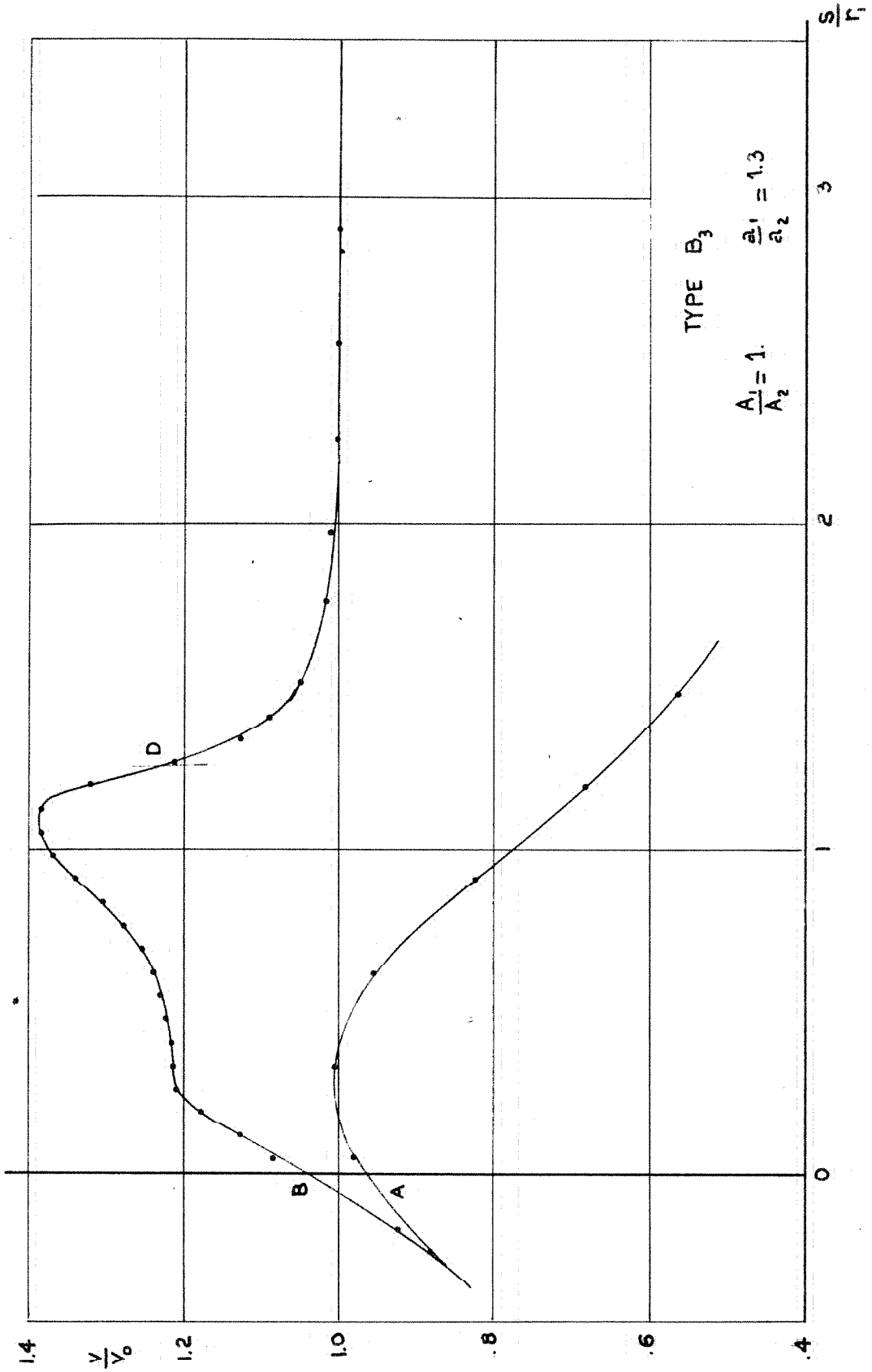

Fig. 18

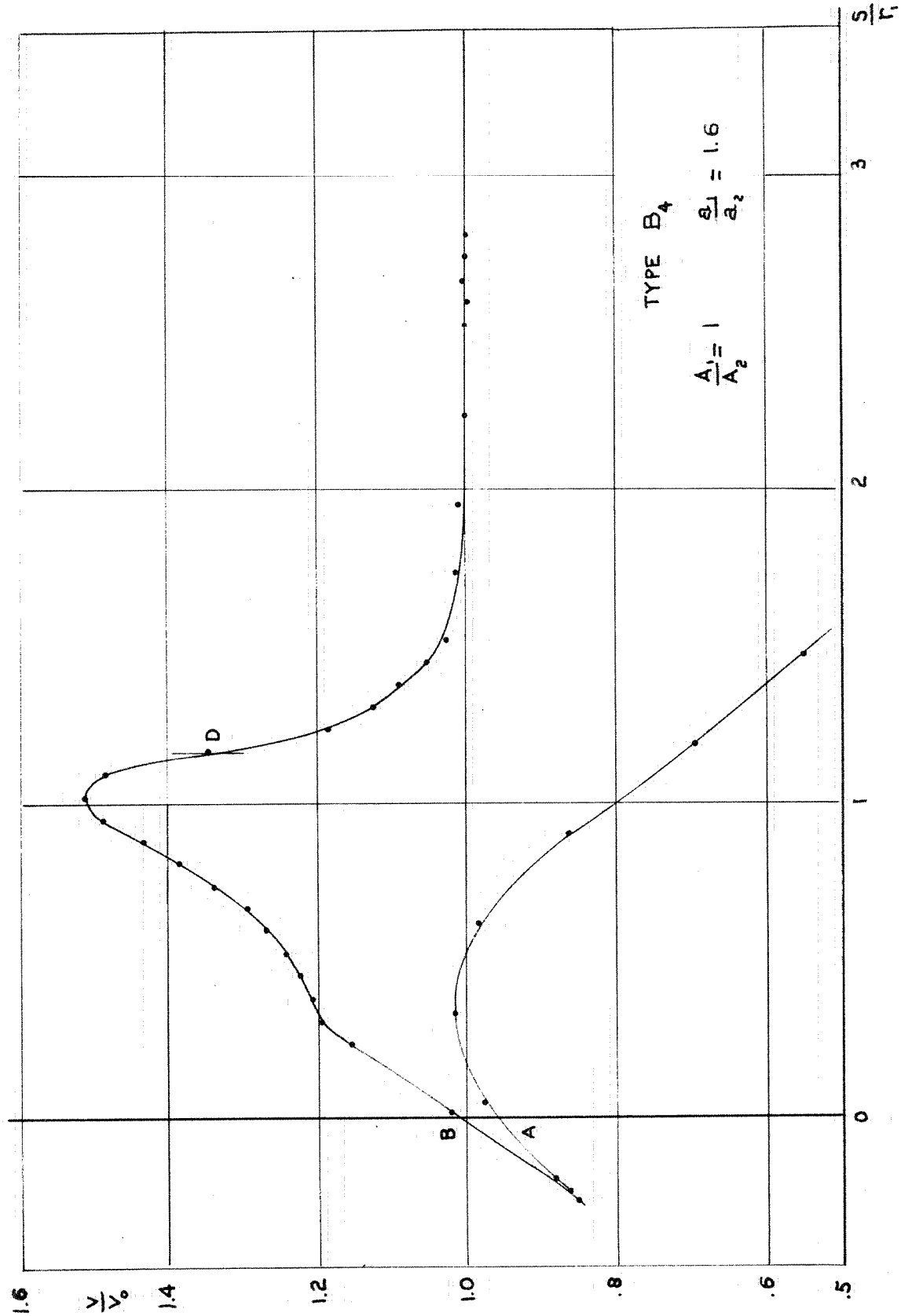

Fig. 19

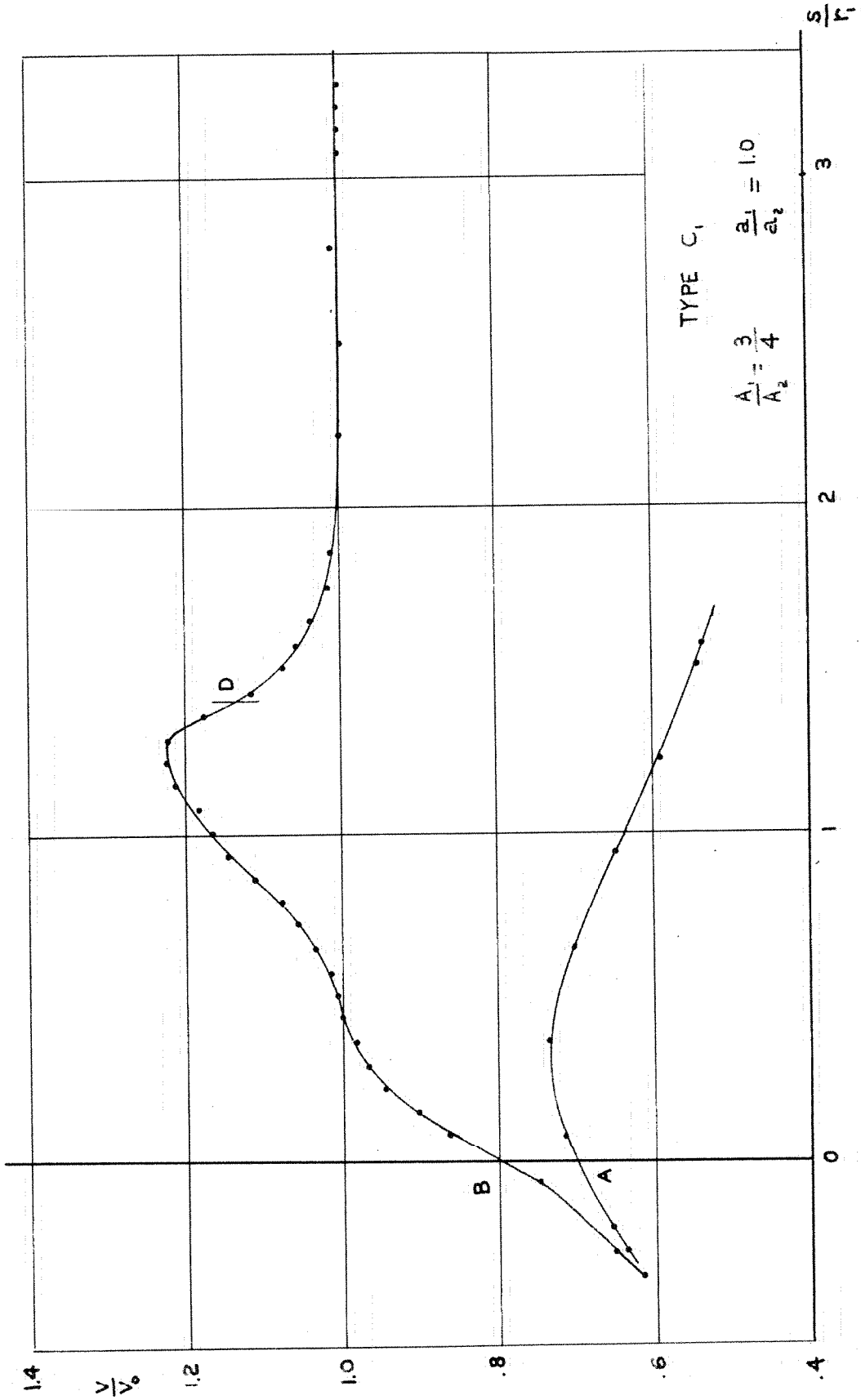

Fig. 20

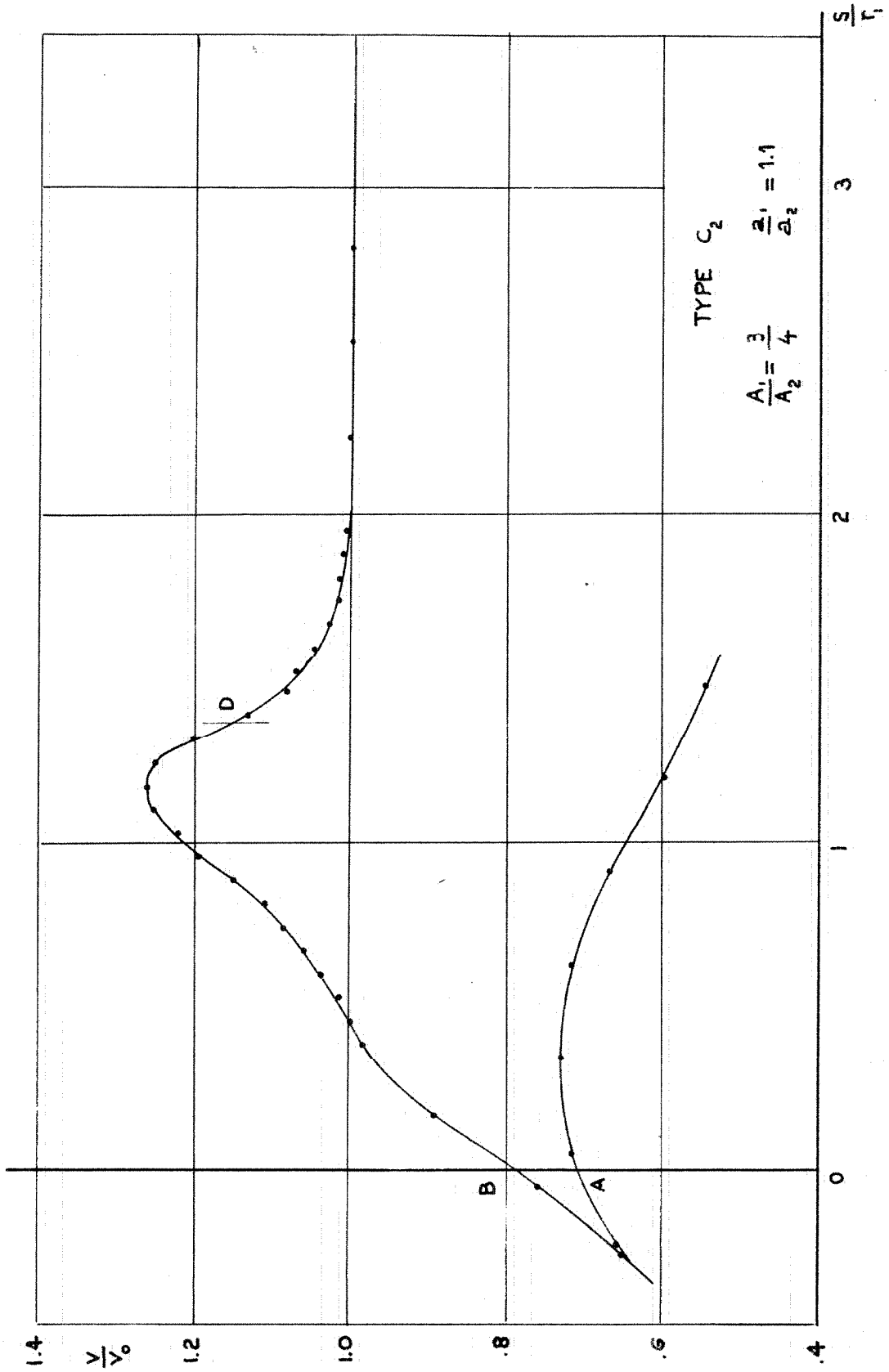
TYPE C_2
$\frac{A_1}{A_2} = \frac{3}{4}$
$\frac{a_1}{a_2} = 1.1$
D
B
A
$\frac{s}{r_1}$
3
2
1
0
1.4
1.2
1.0
.8
.6
.4
$\frac{v}{v_0}$

Fig. 21

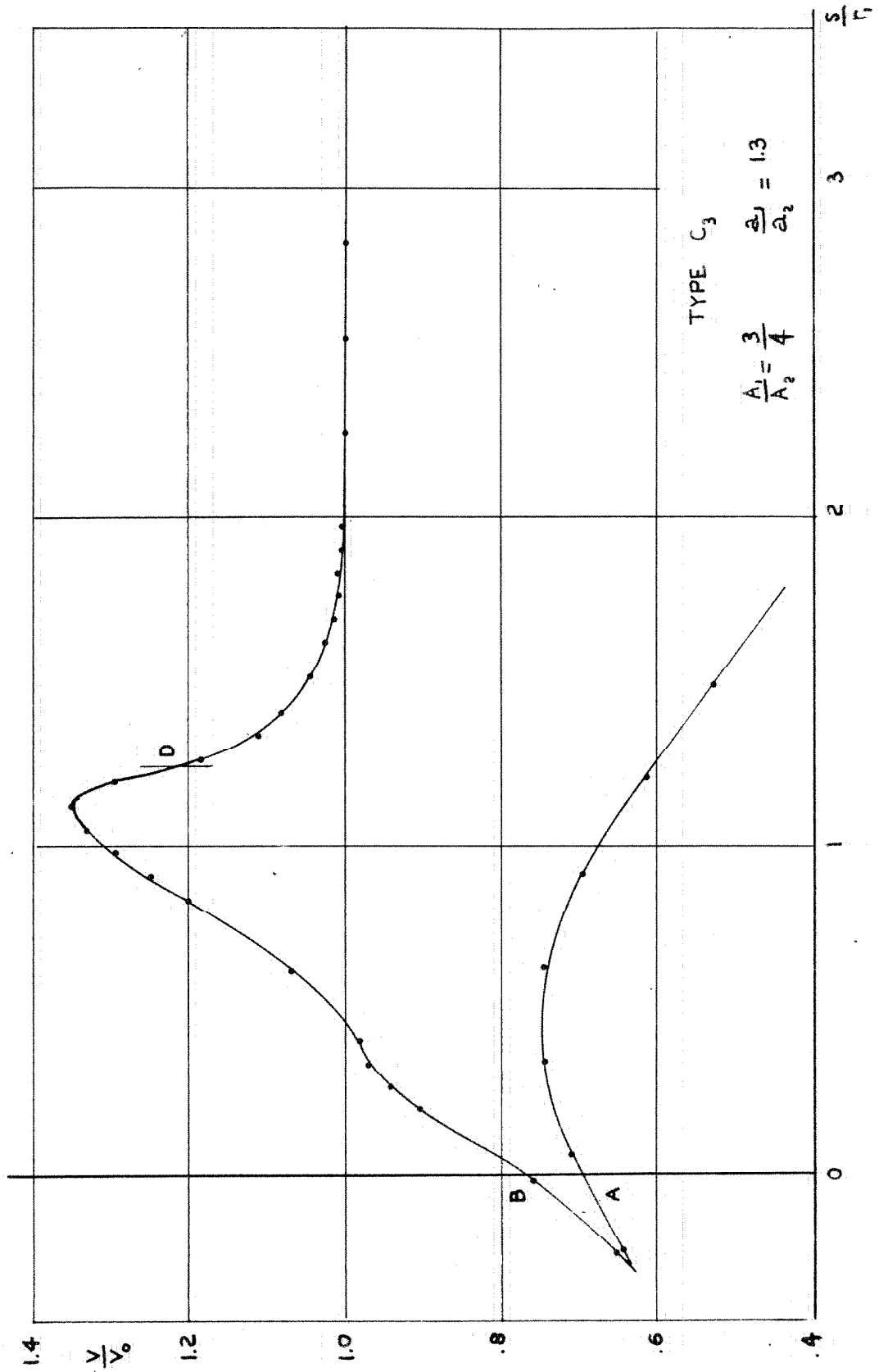

Fig. 22

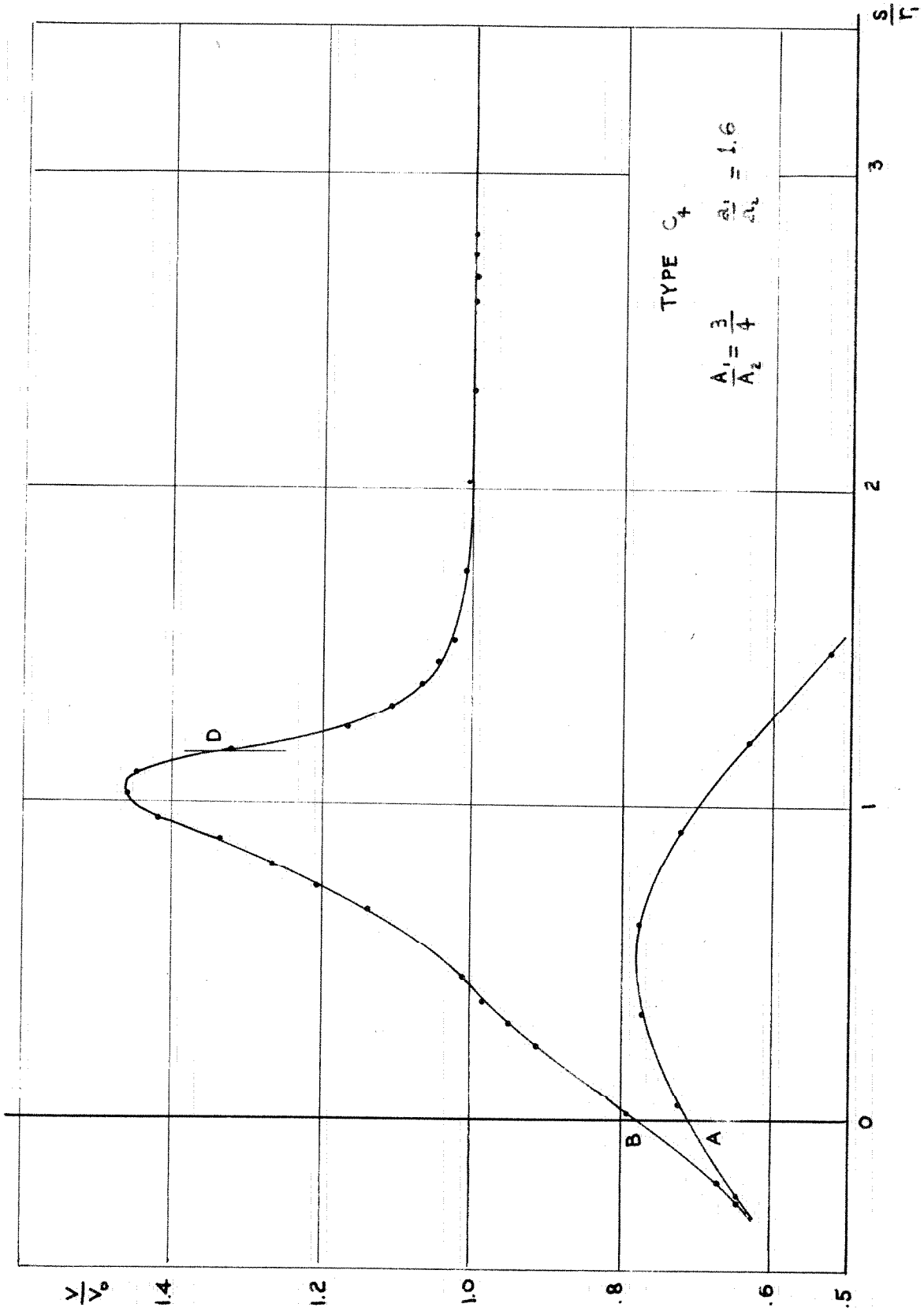

Fig. 23

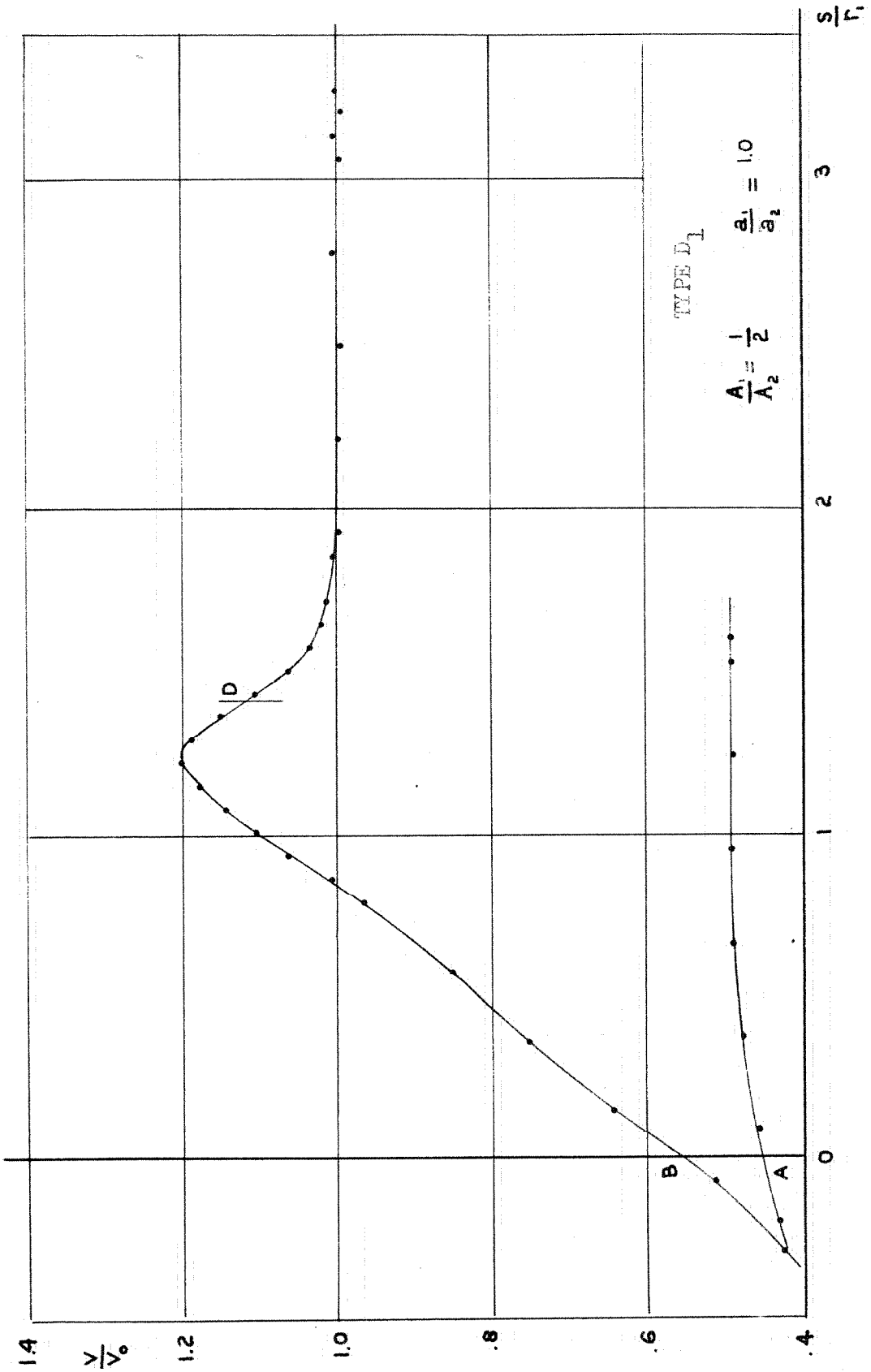

Fig. 24

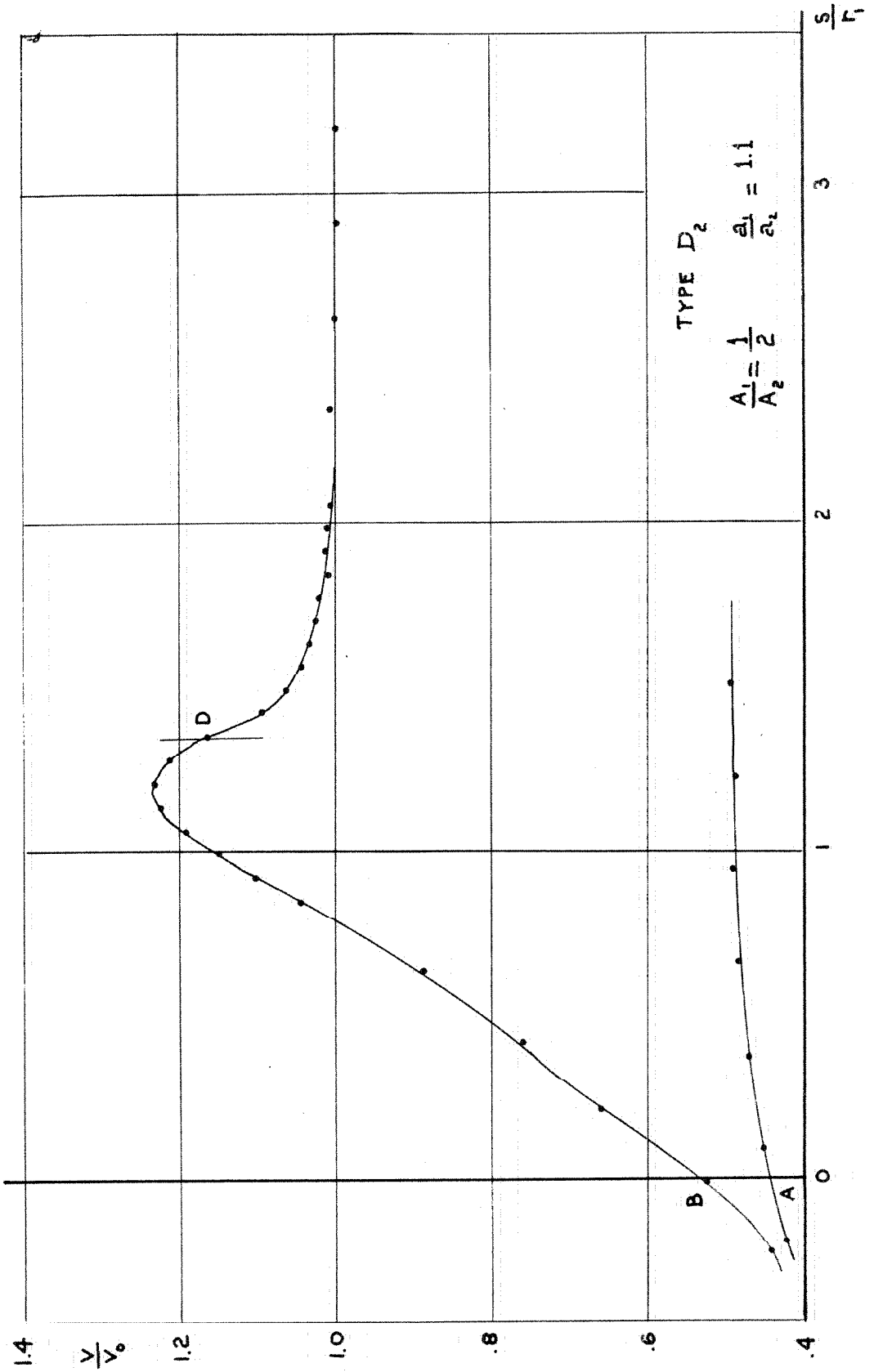
TYPE D_2
$\frac{A_1}{A_2} = \frac{1}{2}$
$\frac{a_1}{a_2} = 1.1$
D
A
B
$\frac{s}{r_1}$
$\frac{v}{v_0}$
0
1
2
3
.4
.6
.8
1.0
1.2
1.4

Fig. 25

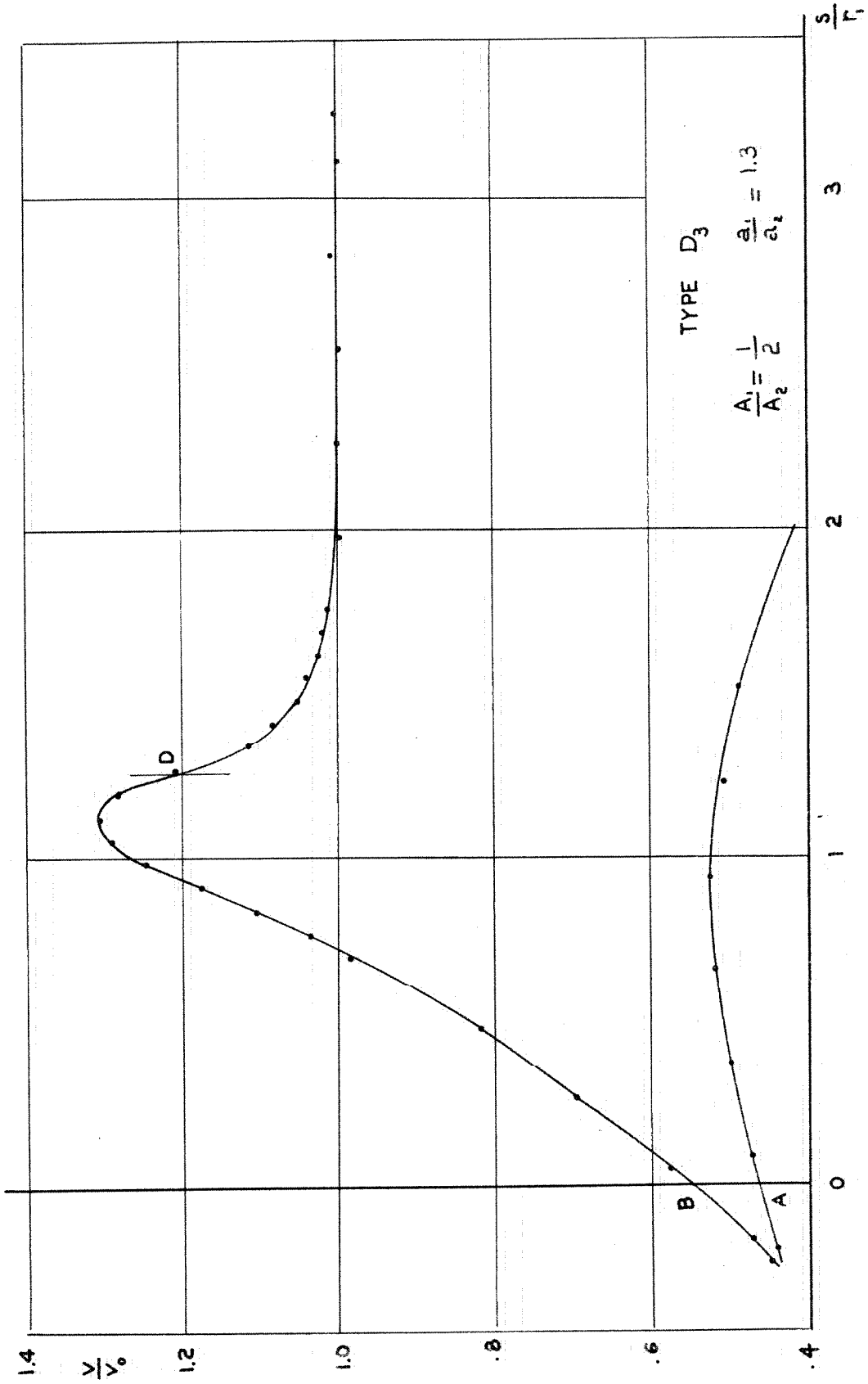
TYPE D_3
$\frac{A_1}{A_2} = \frac{1}{2}$
$\frac{a_1}{a_2} = 1.3$
D
A
B
v/v_0
1.4
1.2
1.0
.8
.6
.4
0
1
2
3
s/r_1

Fig. 26

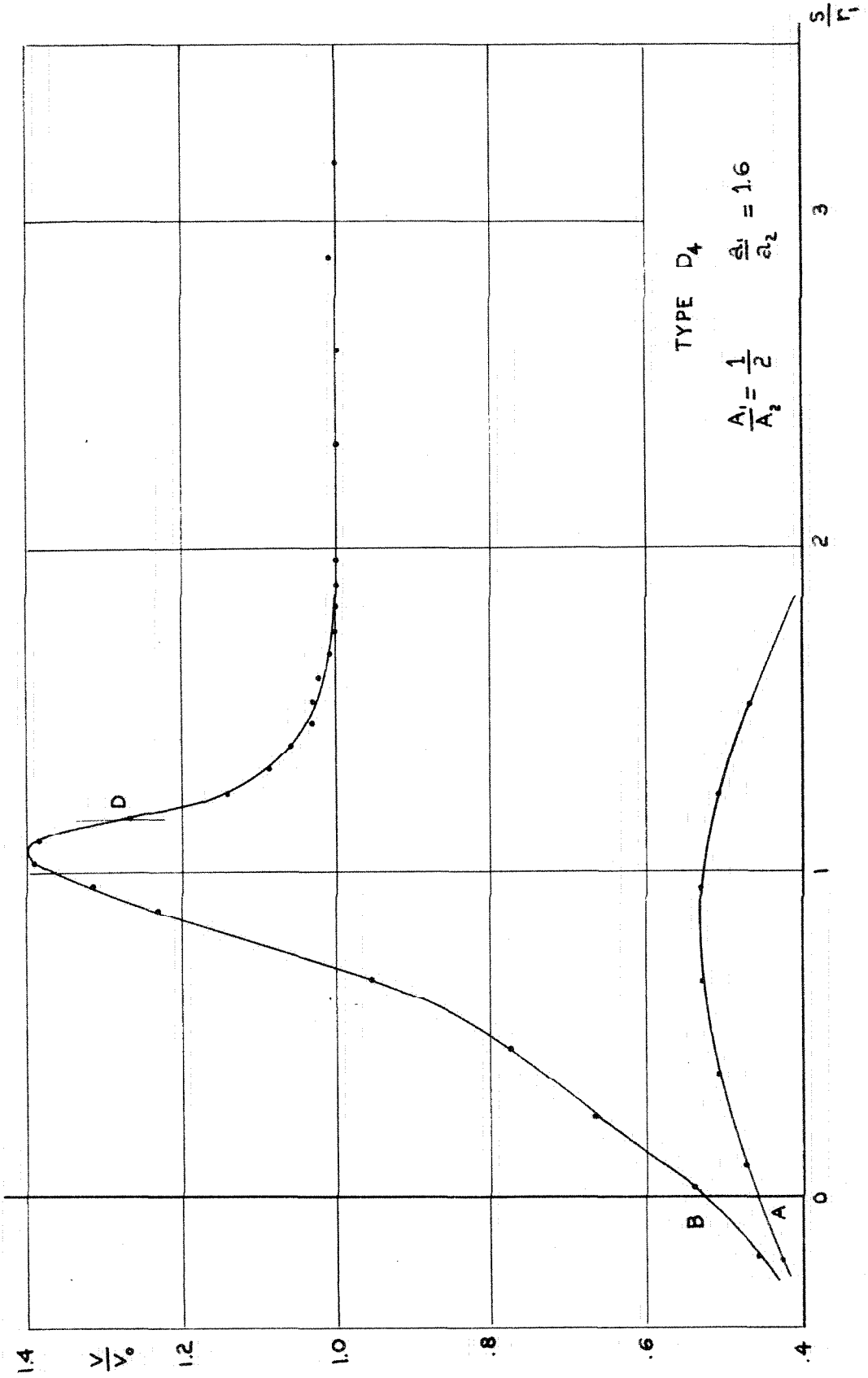

Fig. 27